TU Delft

Delft University of Technology

# Kinetic insights into energy-saving and low-carbon reactive distillation processes for the transesterification to dimethyl carbonate

Xia, Ming; Zhao, Wei; Qi, Xiao-Xiao; Shi, Hui; Cui, Chengtian; Li, Zhikai; Tang, Jihai; Cui, Mifen; Li, Debao; Qiao, Xu

**DOI**
10.1016/j.seppur.2024.129745

**Publication date**
2025

**Document Version**
Final published version

**Published in**
Separation and Purification Technology

**Citation (APA)**
Xia, M., Zhao, W., Qi, X.-X., Shi, H., Cui, C., Li, Z., Tang, J., Cui, M., Li, D., & Qiao, X. (2025). Kinetic insights into energy-saving and low-carbon reactive distillation processes for the transesterification to dimethyl carbonate. *Separation and Purification Technology*, *356*, Article 129745. https://doi.org/10.1016/j.seppur.2024.129745

**Important note**
To cite this publication, please use the final published version (if applicable).
Please check the document version above.

**Copyright**
Other than for strictly personal use, it is not permitted to download, forward or distribute the text or part of it, without the consent of the author(s) and/or copyright holder(s), unless the work is under an open content license such as Creative Commons.

**Takedown policy**
Please contact us and provide details if you believe this document breaches copyrights.
We will remove access to the work immediately and investigate your claim.

*This work is downloaded from Delft University of Technology.*
*For technical reasons the number of authors shown on this cover page is limited to a maximum of 10.*

*Green Open Access added to TU Delft Institutional Repository*

*'You share, we take care!' - Taverne project*

*https://www.openaccess.nl/en/you-share-we-take-care*

Otherwise as indicated in the copyright section: the publisher is the copyright holder of this work and the author uses the Dutch legislation to make this work public.

Separation and Purification Technology 356 (2025) 129745

Contents lists available at ScienceDirect

Separation and Purification Technology

journal homepage: www.elsevier.com/locate/seppur

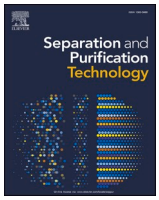

# Kinetic insights into energy-saving and low-carbon reactive distillation processes for the transesterification to dimethyl carbonate

Ming Xia [a,*], Wei Zhao [a], Xiao-xiao Qi [a], Hui Shi [b], Chengtian Cui [c], Zhikai Li [d], Jihai Tang [a], Mifen Cui [a], Debao Li [d], Xu Qiao [a]

[a] State Key Laboratory of Materials-Oriented Chemical Engineering, College of Chemical Engineering, Nanjing Tech University, Nanjing 211816, China
[b] School of Chemistry and Molecular Engineering, Nanjing Tech University, Nanjing 211816, China
[c] Department of Chemical Engineering, Delft University of Technology, Van der Maasweg 9, 2629 HZ, Delft, the Netherlands
[d] State Key Laboratory of Coal Conversion, Institute of Coal Chemistry, Chinese Academy of Sciences, Taiyuan 030001, China

ARTICLE INFO

Editor: Dr. B. Van der Bruggen

*Keywords:*
Catalytic Reactive Distillation
Dimethyl Carbonate
Carbonate
Carbon Neutrality
Investment Reduction
Energy Saving

ABSTRACT

The transesterification of propylene carbonate (PC) or ethylene carbonate (EC) to dimethyl carbonate (DMC) by using catalytic reactive distillation (RD) is a promising approach for carbon dioxide utilization. However, there is still scarcity of comprehensive comparison between the two RD processes. Hence, using the UNIQUAC model and kinetics calibrated by literature and our experiments, we conduct an extensive comparison of the two RD processes. Based on the kinetic insights, laboratory RD processes for both reactions are modeled, analyzed, and experimentally validated. Consequently, two RD processes designed to produce 60 ktpy of DMC are optimized and compared. The interplay and control factors between reaction and separation are elucidated and clarified via investigating variations of the actual chemical equilibrium constant profile compared with theoretical values along the reactive section at various pressures, liquid holdups, etc. The results reveal that the optimized EC RD process achieves almost 50 % reductions in both total annual cost and carbon dioxide emission compared to the PC RD process. This work facilitates the carbon neutrality and provides an essential guide for quantitatively assessing the two routes.

## 1. Introduction

Dimethyl carbonate (DMC) is a well-known environmental-friendly chemical with broad applications due to its negligible ecotoxicity and its biodegradability, being employed as a methylation reagent to substitute extremely toxic dimethyl sulfate (or methyl halides) and as a “green” alternative to acylating agents [1–3]. Additionally, it is also used to produce electrolytes for lithium-ion batteries [4,5].

There are several methods to synthesize DMC, including the phosgenation of methanol (MeOH), oxidative carbonylation of MeOH, direct carbonylation of carbon dioxide with MeOH, and the transesterification method [6,7]. Of all the routes, the former three methods suffer from the obvious drawbacks. Specifically, the phosgenation of MeOH has been forbidden due to environmental constraints, and the oxidative carbonylation of MeOH demonstrates low conversion and challenge in DMC selectivity [6]. The direct carbonylation of carbon dioxide with MeOH commonly faces thermodynamic limitations and remains at the laboratory stage in spite of its advantages such as cheap, abundant, and noncorrosive raw materials and green process [8–10]. Thus, the transesterification method is considered as the most promising and mature route for producing DMC and has been industrialized by companies such as Texaco, Shell, and Mitsubishi Chemical [11,12]. Yet, transesterification is commonly hampered by chemical equilibrium, preventing complete conversion and requires relatively high MeOH to PC or EC ratio. Fortunately, reactive distillation (RD) provides a good selection to overcome the chemical-equilibrium limitation inherent in transesterification that enables continuous and timely removal of the generated products from the reaction system. Main product’s yield of chemical-equilibrium limited reactions such as (trans-)esterification can be significantly increased [13–18]. Hence, RD columns tailored for the transesterification of PC or EC with MeOH can offer significant benefits.

However, RD features that a highly coupled reaction and distillation process within one shell, requiring suitable kinetics and transfer properties to ensure perfect matching between the product formation rate and the distilling rate. Additionally, the homogeneous catalyst, sodium methylate, commonly used in industrial RD brings about the intractable and difficult separation of sodium methylate from the RD bottoms,

* Corresponding author.
*E-mail address:* mxia@njtech.edu.cn (M. Xia).

https://doi.org/10.1016/j.seppur.2024.129745
Received 17 July 2024; Received in revised form 10 September 2024; Accepted 15 September 2024
Available online 24 September 2024
1383-5866/© 2024 Elsevier B.V. All rights are reserved, including those for text and data mining, AI training, and similar technologies.

**Nomenclature**

| | |
|---|---|
| CO | operating cost |
| $c_i$ | concentration of the ith component, kmol·m$^{-3}$ |
| DMC | dimethyl carbonate |
| EC | ethylene carbonate |
| EG | ethylene glycol |
| FCI | fixed capital cost investment |
| ID | inner diameter of column shell |
| $k_{1+}$ | forward reaction rate constant of EC to DMC, s$^{-1}$ |
| $k_{1-}$ | backward reaction rate constant of EC to DMC, m$^3$·kmol$^{-1}$·s$^{-1}$ |
| $k_{2+}$ | forward reaction rate constant of PC to DMC, s$^{-1}$ |
| $k_{2-}$ | backward reaction rate constant of PC to DMC, m$^3$·kmol$^{-1}$·s$^{-1}$ |
| $K_{cs}$ | chemical equilibrium constant based on staged concentration |
| $K_c$ | theoretical chemical equilibrium constant based on the kinetics |
| LPS | low-pressure steam |
| MeOH | methanol |
| $N_R$ | number of rectifying trays |
| $N_S$ | number of stripping trays |
| $N_T$ | number of theoretical stages |
| $N_{RX}$ | number of reactive trays |
| P | operation pressure |
| PC | propylene carbonate |
| PG | propylene glycol |
| R | gas constant, 8.314 J·mol$^{-1}$·K$^{-1}$ |
| RD | reactive distillation |
| $r_{EC}$ | conversion reaction rate of EC, kmol·m$^{-3}$·s$^{-1}$ |
| $r_{PC}$ | conversion reaction rate of PC, kmol·m$^{-3}$·s$^{-1}$ |
| T | temperature, K |
| TAC | total annual cost |
| UNIQUAC | universal quasi-chemical correlation activity coefficient |
| $V_{RX}$ | volume of holdup on the reactive trays |
| $x_{EC}$ | conversion of EC |
| $x_{PC}$ | conversion of PC |

resulting high energy consumption and complex equipment. Heterogeneous catalysts such as anion ion exchange resin, etc. have to be employed or explored [19–23]. However, to date, the enhancement of the reaction rate over heterogeneous catalyst is still quite limited, with the activity of fine heterogeneous catalyst being at most only close to that of sodium methoxide homogeneous catalyst. These can be found in the slurry catalytic RD study by Lv et al. [21] and Yang et al. [22]. Furthermore, the low effectiveness of large catalyst pellet due to the contradiction of reaction rate and column pressure drop reduces apparent reaction rate such that ridiculous large amount of catalyst is required and packed into reactive section of RD column. Hence, homogenous catalyst remains the preferred choice from the standpoint of industrial practice.

Kinetics is one of the most important factors for designing and retrofitting catalytic RD columns. The kinetics of the PC [23] and EC [24,25] transesterification reactions have been systematically studied. Zhang and Luo [23] conducted kinetics experiments and modeling of PC to DMC using sodium methylate solution, achieving an initial reaction rate of around 0.0005 ~ 0.001 kmol m$^{-3}$·s$^{-1}$ under the considered reaction conditions. The proposed kinetics by Zhang and Luo [23] is quite suitable and applicable because the RD simulation results embedded with this kinetics is consistent with the industrial plant data provided by Feiyang Chemical Co., Ltd. (China) [2,3]. For the kinetics of EC to DMC, Fang et al. [24,26] presented a kinetics model, and thereafter performed experimental and simulated studies on RD for DMC synthesis with sodium methylate as the catalyst. Although this kinetics has been extensively used in lots of paper, it suffers from dimensional confusion, namely the rate constants of forward and backward reactions have units of L·mol$^{-1}$·s$^{-1}$ and s$^{-1}$ whereas the unit of kinetics rate is mol·L$^{-1}$·min$^{-1}$. This confusion hinders engineers from quantitively evaluating the rate and may results in poor RD column design. Hence, it is essential to clarify and calibrate the kinetics rate with experimental data.

Vapor-liquid equilibrium (VLE) is the other important factor. The VLE study of the PC to DMC reaction has been well performed by Shi et al. [27], Luo et al. [28,29], and Mathuni et al. [19], achieving excellent consistency between the calculated and experimental VLE according to Huang et al. [2]. As for the EC to DMC reaction, the UNIQUAC model with the built-in binary interaction parameters imbedded in Aspen Plus show excellent agreement between the experimental and calculated VLE. These provide a solid foundation for RD modeling and scale-up.

From the reviews above, it can be retrieved that comprehensive comparisons have never been performed, and that the interplay of kinetics and separation in terms of tray holdup and stages for the two reaction routes have hardly been revealed. Noticed that the differences in kinetics rate of the two reactions brings about differences in tray holdup and stages, suggesting differences in energy consumption, operating and capital investment costs. Furthermore, the papers by Huang et al. [2,3] reported that the bottoms composition of PC is around 1.44 wt%, and therefore a complex hydrolysis process downstream must be set up to remove the unreacted PC. It is undesired because of the potential blockage of equipment due to the precipitation of sodium methoxide. In contrast, the good papers by Fang et al. [26,30] reported that the RD achieves almost total conversion of EC and high selectivity of DMC, consistent with the literature by Asahi Kasei [12,31]. Remarkably and fortunately, there existed only 0.1 wt% EC unreacted in the RD bottoms, potentially avoiding the use of a complex hydrolysis process and preventing blockage. Noticed that only based on the suitable kinetics without confusion, comprehensive comparison should be made. However, there remains lack of calibrated kinetics of EC to DMC and thereafter long-period experimental studies on the validation of RD model. Additionally, sole simulation studies without experimental validation cannot guarantee the reliability of the RD model. In contrast, without the guidance of the modeling and simulation, experiments could be arbitrarily conducted. Therefore, a combined approach of experiment and simulation is employed for this study.

The purpose of this paper is to study the RD of two different routes, reveal the interplay of kinetics and separation in terms of tray holdup and number of stages and make a comprehensive comparison in terms of reaction rates, capital investment and energy costs. Firstly, based on calibrated kinetics, modeling and analysis of the two RD processes are conducted, with the EC to DMC RD model validated in a laboratory RD setup for long-term operation. Secondly, scaled-upped RD processes for producing 60 ktpy of DMC are optimized and discussed in terms of operating pressure, reactive trays, rectifying tray, stripping trays and holdup. Finally, the optimized design for the two RD processes is compared involving economic data, energy consumption and carbon dioxide emission.

## 2. Thermodynamics and kinetics

The homogeneous catalytic RD process, integrating liquid reaction and distillation processes, is notably intricate. This complexity poses challenges when attempting to screen and evaluate different routes. Fortunately, Aspen Plus could provide an effective tool with the steady-state simulation of the DMC synthesis within a RD column.

**Table 1**
Binary Interaction Parameters $a_{ij}$ and $b_{ij}$ of the UNIQUAC Model for the PC to DMC.

| Comp. i | MeOH | DMC | DMC | PG | MeOH | MeOH |
|---|---|---|---|---|---|---|
| Comp. j | DMC | PC | PG | PC | PG | PC |
| $a_{ij}$ | 7.061 | 0 | 0 | 0 | 0 | 0 |
| $A_{ji}$ | −8.109 | 0 | 0 | 0 | 0 | 0 |
| $b_{ij}$ (K) | −2395.356 | 172.470 | −209.529 | −290.492 | −301.778 | 49.94 |
| $B_{ji}$ (K) | 2457.924 | −216.199 | −9.027 | 59.416 | 142.266 | −244.595 |

**Table 2**
Binary Interaction Parameters $a_{ij}$ and $b_{ij}$ of the UNIQUAC Model for the EC to DMC.

| Comp. i | MeOH | DMC | DMC | EG | MeOH | MeOH |
|---|---|---|---|---|---|---|
| Comp. j | DMC | EC | EG | EC | EG | EC |
| $a_{ij}$ | 0.30356 | 0.45281 | 3.3311 | −9.07962 | −30.0441 | 2.73049 |
| $A_{ji}$ | 1.12075 | 0.14056 | −1.6368 | 8.92515 | 2.8879 | −2.34082 |
| $b_{ij}$ (K) | −89.351 | −682.682 | −1430.12 | 3627.65 | 9254.07 | −1102.64 |
| $B_{ji}$ (K) | −700.786 | 148.446 | 429.06 | −3873.45 | −822.92 | 743.732 |

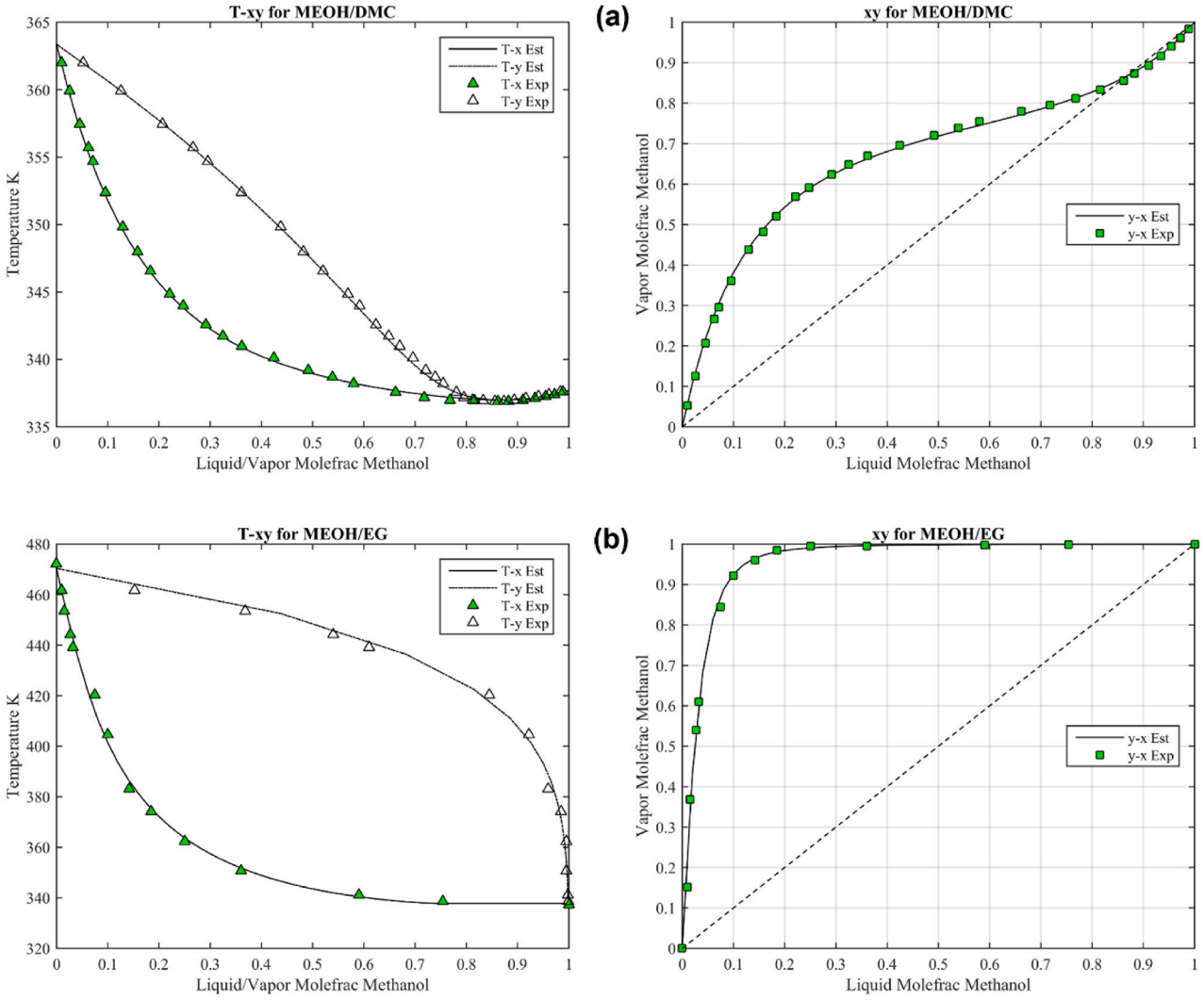


**Fig. 1.** Experimental and estimated T-xy and y-x at corresponding pressure: ((▲, △, ■)) experimental data from the literature; (—,·—·) estimated data by the UNIQUAC model. (a) MeOH and DMC at 101.3 kPa; (b) MeOH and EG at 101.3 kPa; (c) MeOH and EC at 101.3 kPa; (d) DMC and EG at 35.33 kPa; (e) DMC and EC at 101.3 kPa; (f) EG and EC at 6.87 kPa.

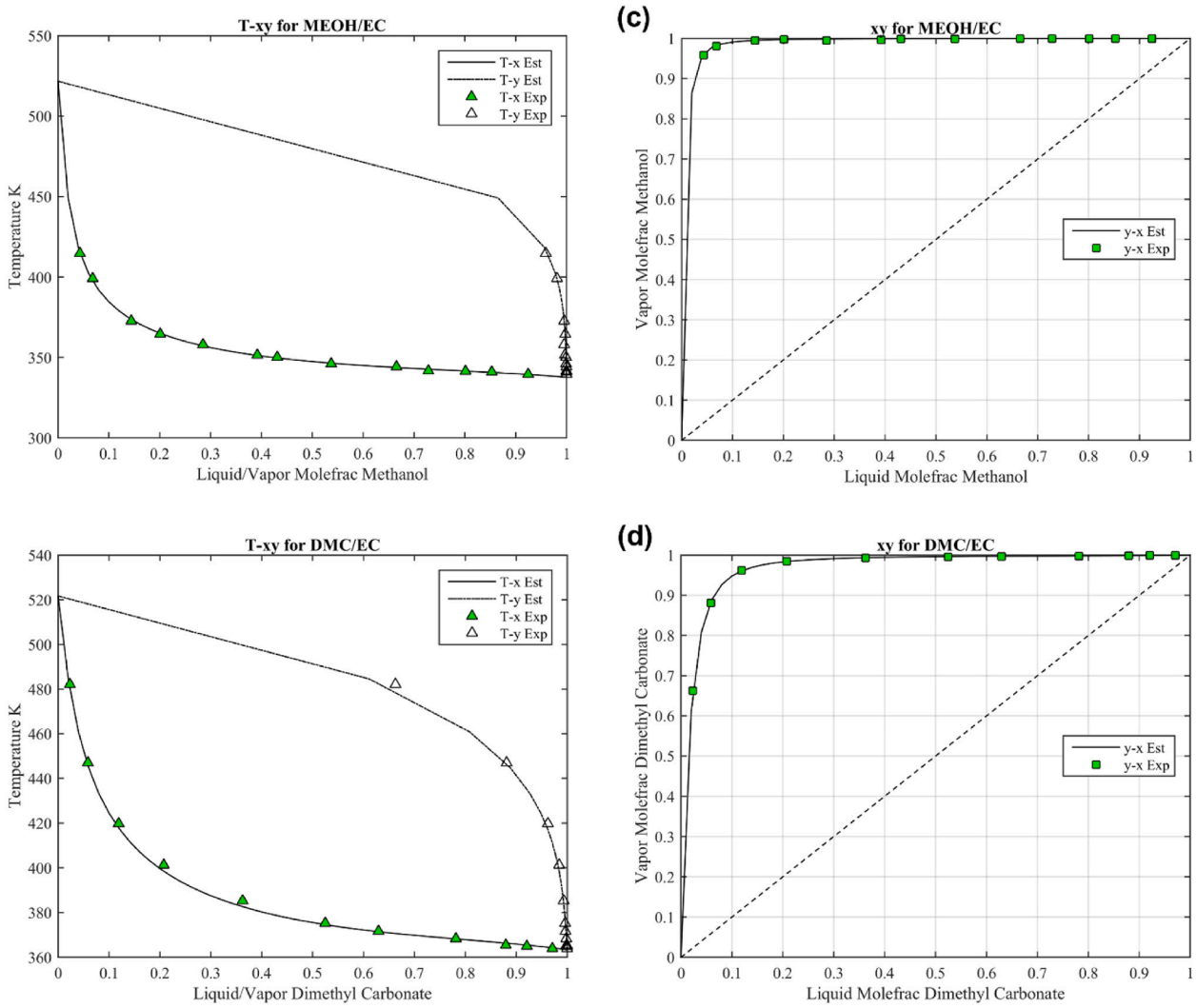


**Fig. 1.** (*continued*).

### 2.1. Thermodynamics Property

Both the EC to DMC and PC to DMC routes encompass four components, namely EC to DMC (MeOH, EC, DMC, and EG) and PC to DMC (MeOH, PC, DMC, and PG). Noticed that MeOH and DMC form a minimum-boiling azeotrope with a composition of 0.67/0.33 wt/wt at 101.3 kPa. Therefore, it becomes quite significant to select suitable thermodynamics properties that accurately describe the VLE of the both quaternary systems.

For the PC to DMC RD, the UNIQUAC model for the liquid phase and the RK model for the vapor phase are used to describe the vapor–liquid equilibrium (VLE). Regression was performed based on the experimental vapor–liquid equilibrium data. The experimental data for the MeOH/DMC pair are retrieved from Rodríguez et al. [32]. The binary interaction parameters of DMC/PC, DMC/PG and PG/PC identical to Huang et al. [2] are regressed with the experimental data from Luo et al. [29] and Mathuni et al. [19], and other binary interaction parameters of MeOH/PG, MeOH/PC are directly retrieved from Huang et al. [2] because of their perfect simulations. All the binary interaction parameters listed in Table 1 offer good agreements between the experimental and estimated VLE as in Figure S1 (SI). For the EC to DMC RD, the UNIQUAC model for the liquid phase with idea gas model are used to describe the VLE. The binary interaction parameters of MeOH/DMC, MeOH/EG, MeOH/EC, DMC/EG, DMC/EC, and EG/EC retrieved from the Aspen Plus are listed in Table 2 because of the excellent agreements [30,32,33] between the experimental and estimated VLE (Fig. 1).

### 2.2. Catalysis and kinetics

The catalytic kinetics of PC with MeOH using sodium methoxide as catalyst has been studied by Zhang et al. [23]. However, although Fang et al. [24] has proposed the kinetics of EC with MeOH using sodium methoxide as catalyst and reported a good agreement with the simulated results of laboratory-scale RD, there still existed a problem of dimensional confusion, namely the rate constant of forward and backward reaction units is as $L{\cdot}mol^{-1}{\cdot}s^{-1}$, and $s^{-1}$ whereas the unit of kinetics rate is as $mol{\cdot}L^{-1}{\cdot}min^{-1}$. Hence, we perform experiment using a three-neck flask to verify and calibrate the kinetics rate based on Fang's [24]. It is disclosed as compared in Fig. 2 that the calibrated rate constant is around 60 times higher than that by Fang's, and thus for simple transformation the unit of kinetics rate of EC consumption should be $kmol{\cdot}m^{-3}{\cdot}s^{-1}$, but not $kmol{\cdot}m^{-3}{\cdot}min^{-1}$. Thus, the both transesterification reactions are reversible with corresponding suitable kinetics expressed as follows:

(1) EC to DMC reaction:

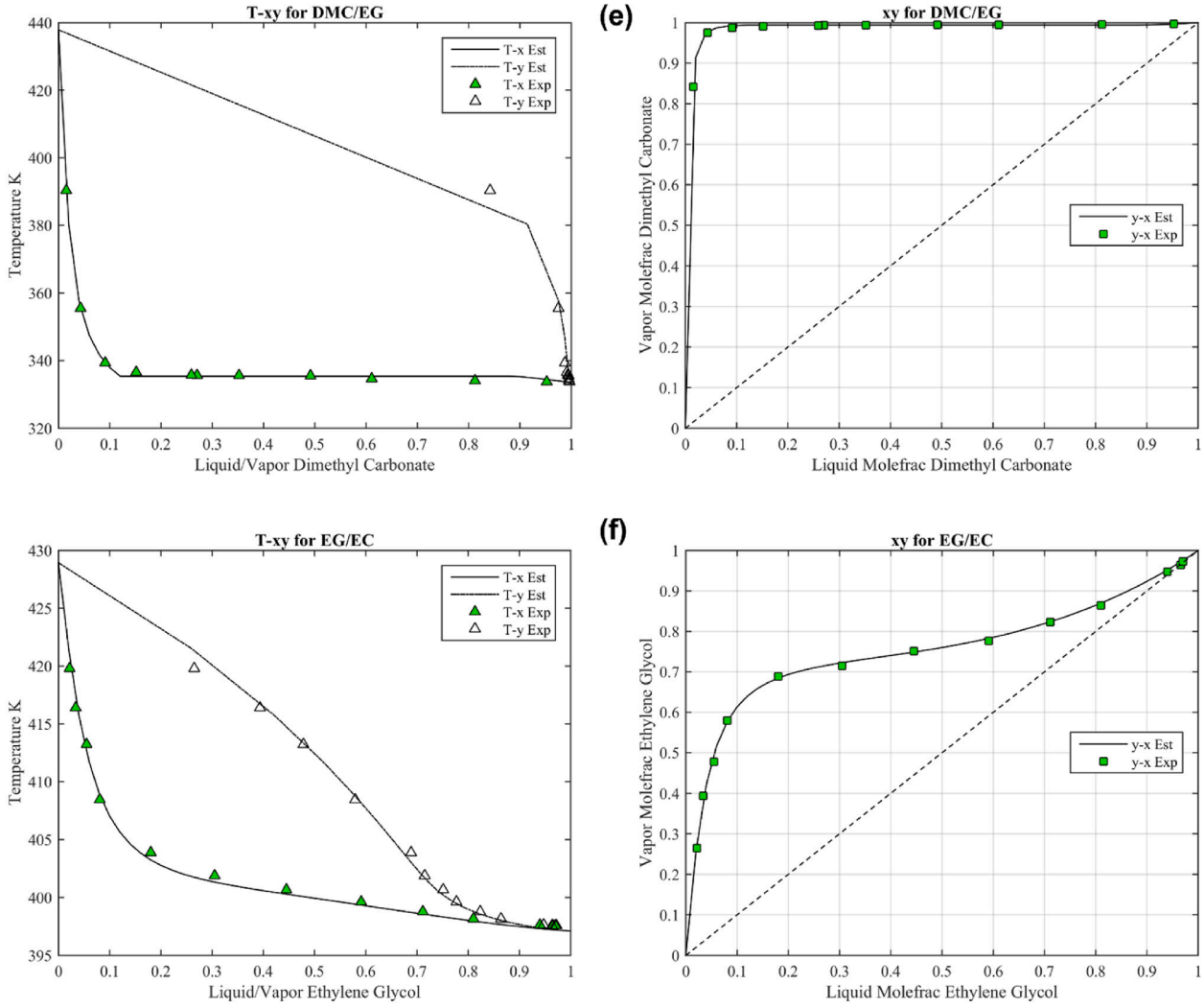


**Fig. 1.** (*continued*).

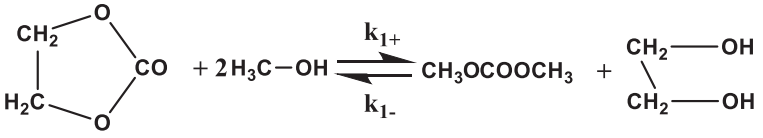


**EC** **MeOH** **DMC** **EG**

Reaction 1

$$r_{EC} = k_{1+}c_{EC}c_{MeOH} - k_{1-}\frac{c_{DMC}c_{EG}}{c_{MeOH}} \quad (1)$$

$$k_{1+} = 1.3246\exp\left(\frac{-13060}{RT}\right) \quad (2)$$

$$k_{1-} = 15022\exp\left(\frac{-28600}{RT}\right) \quad (3)$$

(2) PC to DMC reaction:

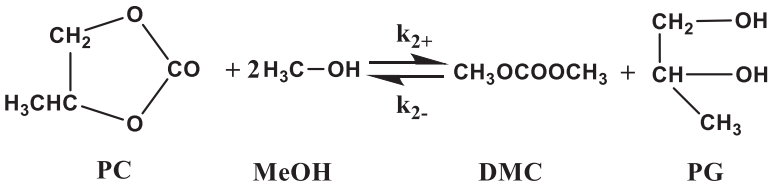


Reaction 2

$$r_{PC} = k_{2+}c_{PC}c_{MeOH} - k_{2-}\frac{c_{DMC}c_{PG}}{c_{MeOH}} \quad (4)$$

$$k_{2+} = 275.86\exp(\frac{-41373.5}{RT}) \quad (5)$$

$$k_{2-} = 320.91\exp(\frac{-28285.5}{RT}) \quad (6)$$

where $r_{EC}$, $r_{PC}$ is conversion reaction rate of EC, PC, respectively (kmol·m$^{-3}$·s$^{-1}$), $c_i$ is concentration of the ith component (kmol·m$^{-3}$), T is reaction temperature (K), R is the gas constant (R=8.314 J·mol$^{-1}$·K$^{-1}$). Based on the kinetics by Fang et al. [26] at sodium methylate concentration (proportion of pure sodium methylate weight to total weight of sodium methylate and methanol) of 0.2 to 0.30 wt%, the kinetics rate is calibrated by our experiment at 437.15 K and identical catalyst concentration, it is proven that the time unit related the kinetics should be second rather than minute. Meanwhile, the kinetics expression for PC conversion obtained by the experiment catalyzed by sodium methylate concentration of 0.4 to 0.45 wt% [23]. Thus, it is reasonable to ignore the catalyst component in the simulation for simplification.

### 2.3. Kinetic insights

The conversion of EC, or PC with the temperature at various reaction rates for given feed ratio (MeOH/EC or PC) are calculated as in Fig. 3 and Fig. 4 by using the corresponding kinetics equations. The higher the feed ratio, the higher conversion at the given temperature and reaction rate for the both reactions, suggesting the optimized feed ratio exceeding 9/1 mol/mol should be essential.

The EC to MeOH exhibits the characteristic figure for typical reversible exothermic reaction as in Fig. 3. For each reaction rate the EC conversion gradually decreases with temperature, and thus a moderate low temperature should be good. Meanwhile, considering the boiling point of MeOH, EC, EG and the singular point of the system as shown in Table 3, temperature range of 336 ~ 348 K should be quite beneficial for the EC conversion and achieving vapor–liquid flow through RD column.

However, for the PC to MeOH the trends violate the typical reversible exothermic reaction but obey the typical reversible endothermic reaction as in Fig. 4. In spite of the abnormality, this kinetics can perfectly describe this reaction with accordant simulations [2,23]. For each reaction rate, PC conversion increases with temperature, and accompanied with the singular points as listed in Table 4, a relatively high reaction temperature range of 336 ~ 353 K should be preferred for both PC conversion and excellent vapor–liquid flow within RD column.

At a relatively high EC conversion of 85 % and 336 ~ 348 K, the EC conversion rate (~0.03 kmol m$^{-3}$ s$^{-1}$) is around 30 times higher than the PC conversion rate (~0.001 kmol m$^{-3}$ s$^{-1}$) at its conversion of 70 % and 336 ~ 353 K. This suggests the reaction rate of EC conversion is much faster and more sufficient compared with those of the PC conversion, implying a much less liquid holdup in the reactive section if the RD column is employed.

## 3. Modeling, simulation and experiment

The RadFrac module based on the rigorous equilibrium stage model considers mass, energy balance, summation, and phase equilibrium equations. The equilibrium stage model is chosen in the RadFrac module since it has been successfully applied in the modeling of lots of RD processes acetic acid esterification [36,37], etherification such as TAME [38], MTBE [39], etc.

As sketched in Fig. 5, for the both transesterification RD, there are three streams, namely MeOH flow, PC (or EC) flow, and CAT flow using sodium methoxide saluted in methanol. The PC (or EC) flow and the CAT flow are both fed to the upper of the column, while the MeOH flow to the lower of the column. Thus, the column is divided to three sections, rectifying section (above the PC or EC flow feeding location), reactive section (between the MeOH flow and the PC or EC flow feeding locations), and stripping section (below the MeOH flow feeding location). The reactive section offers sufficient contact surface for the transesterification reaction to generate DMC and EG, in which an azeotrope of DMC/MeOH is formed and ascended to the top while the higher boiling EG drops into the bottoms. The function of the rectifying section is to achieve the separation of PC or EC and the DMC/MeOH azeotrope, assuring the least PC or EC ascending to the overhead flow. The stripping section strips the DMC and the excessive MeOH descends from the reactive section.

As shown in Fig. 6 and Table 5, a RD column with a height of 1930 mm Dixon (also called theta circle in China, 2 mm × 2 mm, ~ 30 theoretical stages per 1000 mm) dumped packing are built and operated to validate the laboratory RD model for the transesterification of EC to DMC. The transesterification of EC to DMC RD experiments are not scheduled because of the excellent simulation in good agreements with the plant data according to Huang et al. [2].

### 3.1. Laboratory RD simulation and validation

Based on the analysis above, we model continuous laboratory RD processes for the two reactions. With the thermodynamics and kinetics given in the Section 2 imbedded in the RadFrac block in Aspen Plus V12.1, two RD models with corresponding process parameters can be established as listed in Fig. 5. Since the laboratory column only has an inner diameter of ~32 mm and can only undertake ~ kg/h liquid or vapor flowrate, initially the fresh PC or EC mass flowrate is set at 1.5 g/min with a temperature of 333.15 K and the MeOH flowrate is ~3.87 (molar ratio of MeOH: EC or PC=10: 1) times the PC or EC mass flowrate and specified at ~5.8 g/min with a temperature of 337.15 K. The overhead pressure is specified at 101.33 kPa also according to the laboratory column practice, with a rough pressure drop of 40 kPa.

The interplay among liquid holdup, stages of reactive section, and reflux ratio commonly plays important influence on RD column, especially for homogeneous reaction, as recommended by Luyben and Yu [40]. Liquid holdup and stages of reactive section directly affect quantity of liquid involved in the reaction, while reflux ratio directly affect separation degree in distillation. The balancing and matching of the three parameters determine status of RD. Herein, we have specified a roughly sufficient stages of reactive section, hence the influence of liquid holdup and reflux ratio on reaction and separation could be quantitively investigated.

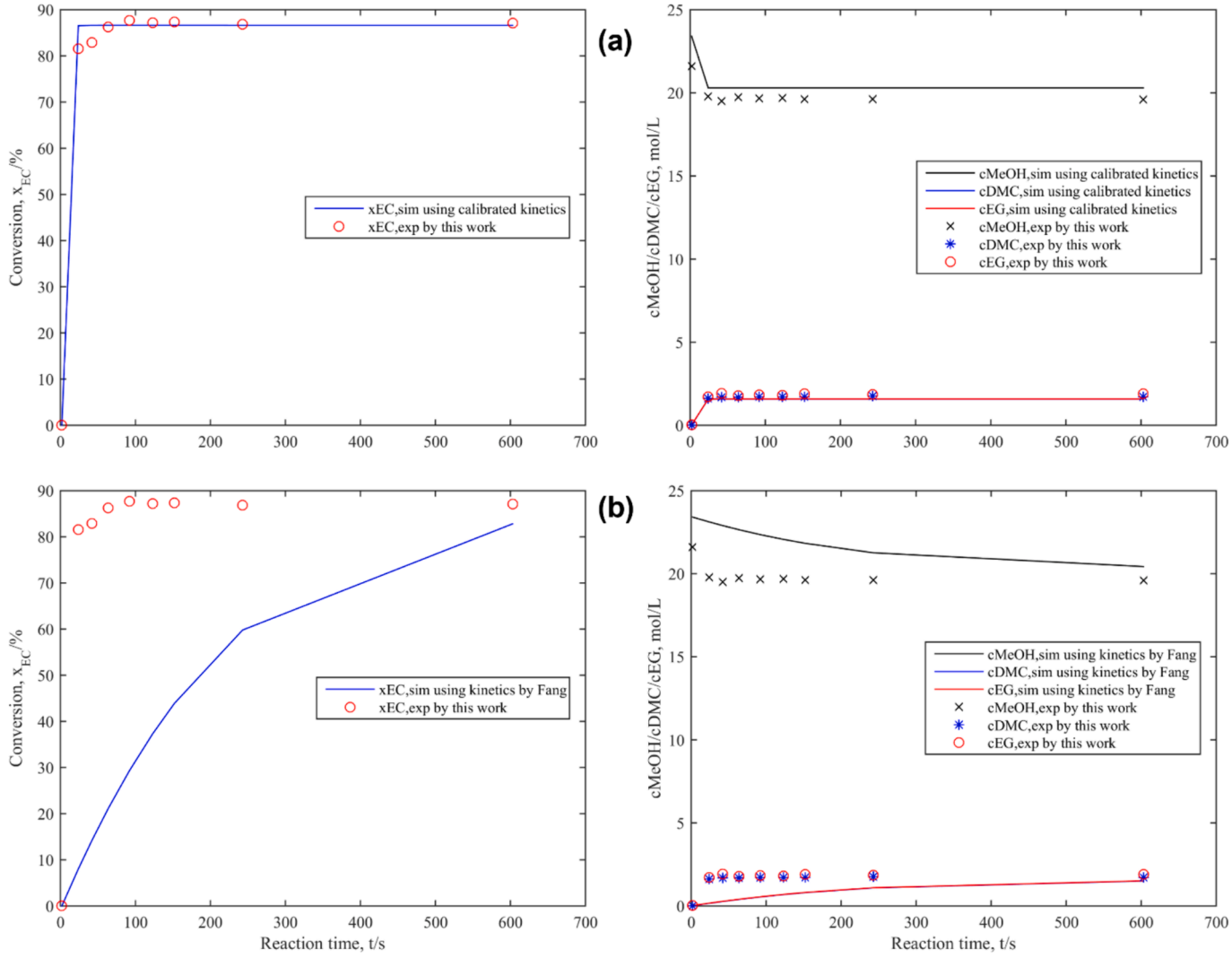


**Fig. 2.** The simulated results related to conversion and concentrations with reaction time at a sodium methylate concentration of 0.25 wt% in terms of the total feed (a) using calibrated kinetics and (b) using the kinetics by Fang et al. [24] in comparison with experimental data by this work at 437.15 K and atmospheric pressure.

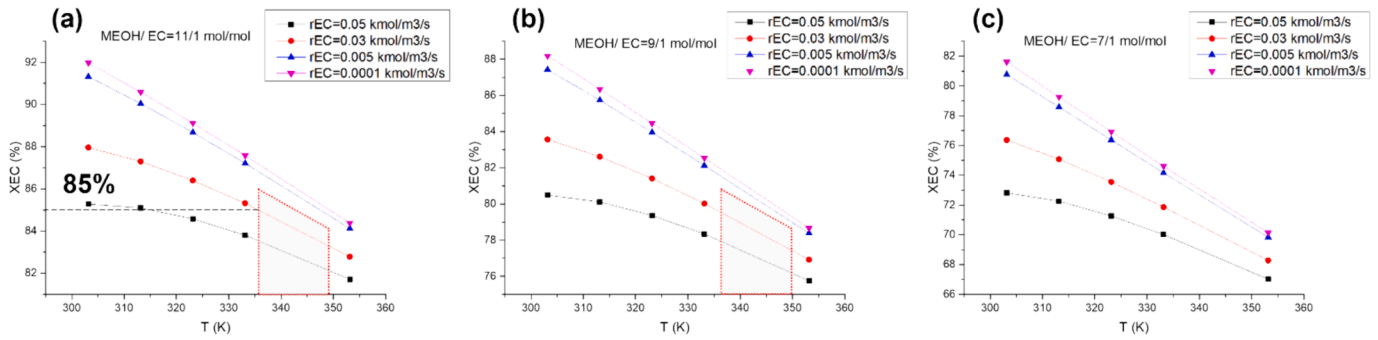


**Fig. 3.** EC conversion with temperature at various EC consumption rates.

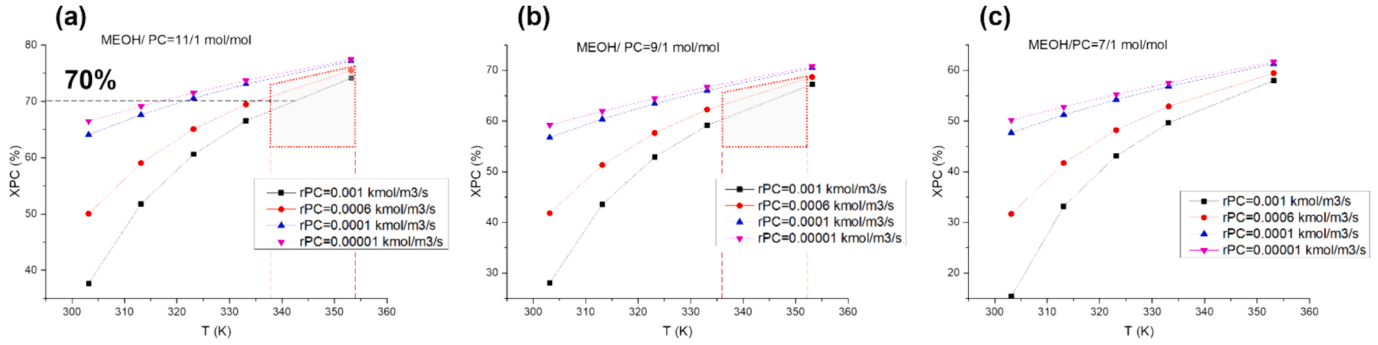


**Fig. 4.** PC conversion with temperature at various PC consumption rates.

### 3.2. EC to DMC

***Simulated Analysis.*** Fig. 7 shows that EC conversion, DMC content in distillate, recovery of DMC generated, and EC content in bottoms show a plateau as mass reflux ratio increase from 0.4 to 0.8, then the former three indexes gradually decrease while the EC content in bottoms gradually decreases as reflux ratio increase from 0.8 to 5. Fortunately, only a low liquid holdup of 2 mL with a 0.8 lower reflux ratio is required to achieve EC conversion of 99.9 % (Fig. 7**a**). This is mainly due to the quite high reaction rate of EC to DMC. It is also revealed that for a given holdup only a small reflux ratio is required to achieve the highest EC conversion, lowest EC content in the bottoms, highest DMC content in the distillate (nearly azeotropic composition), and the highest recovery of DMC generated. This suggests that the reaction rate is sufficiently high such that distilling rate could be a limited factor at higher reflux ratios, hence a small reflux ratio could guarantee the timely removal of the generated DMC from the overhead. Hence, liquid holdup per stage (2 mL/1 stage) multiplies the stages of reactive section (30) produces a total liquid holdup of 70 mL, exceeding which a satisfied reaction effect could be obtained. The holdup of 2 mL per stage should be appropriate, as the column diameter, determined by the maximum raising vapor, can accommodate this holdup effectively.

**Table 3**
Singular points of the EC to DMC system.

| node | type | component | boiling point, K | composition, wt/wt |
|---|---|---|---|---|
| | | | Est. (Exp.) | Est. (Exp.) |
| azeotrope | unstable | methanol/ dimethyl carbonate | 337.0 (336.9) [32] | 0.695/0.305 (0.669/0.331)[32] |
| MeOH | saddle | methanol | 337.7 (337.7) [34] | 1 |
| DMC | saddle | dimethyl carbonate | 363.4 (363.4) [34] | 1 |
| EG | saddle | ethyl glycol | 470.4 (471.0) [34] | 1 |
| EC | stable | ethylene carbonate | 521.7 (516.7 at 0.987 bar) [35] | 1 |

***Experimental Validation.*** In order to validate the laboratory RD model, a column was built and operated as shown in Fig. 6 and detailed in Table 5. The total stages are around 60 with ~ 30 reactive stages. Fresh EC (along with the CAT flow) and fresh MeOH flow were roughly fed to stage 16 and 46 respectively according to the boiling points and densities of the feed components. The overhead pressure was naturally maintained at atmospheric pressure, in line with laboratory column practice. The experimental start up and operation is as in Section 1 (see SI).

A long-term steady operation of the RD column, exceeding 400 h, was carried out. Comparisons at four points indicated that the model could accurately simulate the experimental results, including flowrates, compositions of the distillate and bottoms, temperatures of the top and reboiler, and the EC conversion as listed in Table 6. Since only the reversible transesterification reaction is considered, the selectivity cannot be rigorously simulated. In summary, the model of the transesterification reaction should be competent in process/engineering design of the scaled-up RD systems, provided the contradiction of liquid holdup and tray drop is well addressed.

### 3.3. PC to DMC

***Modeling.*** The influence of reflux ratio with various liquid holdup on PC conversion, PC content in bottoms, DMC content in distillate, and recovery of DMC generated is depicted in Fig. 8. It is revealed that a quite high liquid holdup exceeding 50 mL with a 0.8 higher reflux ratio is required to achieve PC conversion of 97 % due to the low reaction rate of PC to DMC (Fig. 8**a**). There exists an optimum reflux ratio for a given holdup that achieve the highest PC conversion, the lowest PC content in the bottoms, the highest DMC content in the distillate (nearly azeotropic composition), and the highest recovery of DMC generated. Hence, liquid

**Table 4**
Singular points of the PC to DMC system.

| node | type | component | boiling point, K | composition, wt/wt |
|---|---|---|---|---|
| | | | Est. (Exp.) | Est. (Exp.) |
| azeotrope | unstable | methanol/ dimethyl carbonate | 336.8 (336.9) [32] | 0.681/0.319 (0.669/0.331)[32] |
| MEOH | saddle | methanol | 337.7 (337.7) [34] | 1 |
| DMC | saddle | dimethyl carbonate | 363.4 (363.4) [34] | 1 |
| PG | saddle | 1,2-propanediol | 460.8 (460.5) [34] | 1 |
| PC | stable | propylene carbonate | 515.0 (515.2) [35] | 1 |

holdup per stage (50 mL/1 stage) multiplies the stages of reactive section (35 stages) produces a total liquid holdup of 1750 mL, exceeding which a satisfied reaction effect could be obtained. However, the holdup of 50 mL per stage probably is too large such that the diameter of column, determined by merely raising vapor, cannot offer this large holdup. Noticed that the holdup of 50 mL per stage is mainly based on the assumed specified parameters to achieve the targeted indices. Further optimizing the operation pressure, numbers of reactive, rectifying and stripping trays, and even adjusting the column two-end specifications can reduce the holdup to an attainable value.

## 4. Scaled-up process studied

Once the laboratory scale models have been established and validated, we explore a scaled-up processes with a production capacity of 60 ktpy of DMC (120 % overdesign) is explored with the consideration of 1 million tons per year more marketing of the DMC. Based on the laboratory RD model, the EC to DMC RD is magnified around 133,627 times and the PC to DMC RD process is magnified around 95,079 times relative to the corresponding laboratory scale. Since holdup is proportional to DMC production and liquid height on tray according to analysis in Fig. 9, the ratio $\frac{P_{SU}}{P_{Lab}}$ of scaled-up DMC production to laboratory DMC production multiplies the ratio $\frac{h_{liquid,SU}}{h_{liquid,Lab}}$ of liquid height to laboratory liquid height could be assumed as magnifying factor, and thus holdup per tray is roughly 13.4 $m^3$ (2 mL × 133,627 × 50) for the EC to DMC and 47.6 $m^3$ (50 mL×95,079 × 10) for the PC to DMC process. Although these values appear excessively large, they can further be optimized. The initial design parameters remain consistent with the laboratory RD model as in Fig. 5.

Based on the models, it should be quite convenient and efficient to optimize the scaled-up processes in terms of energy consumption, product loss, and product flowrate by considering the effects of various parameters such as pressure (P), number of column trays ($N_T$), number of reactive trays ($N_{RX}$), number of stripping trays ($N_S$), number of rectifying trays ($N_R$), holdup on the reactive trays ($V_{RX}$).

### 4.1. Economic and $CO_2$ emissions basis

In the overall chemical process design, our primary concern lies in the economic comparison between the both RD processes. Prior to the comparison, we only adjust the key parameters above to seek the optimized design for simplicity. The total annual cost (TAC) proposed by Douglas [41] is employed to evaluate chemical engineering designs.

$$\mathrm{TAC}\left(\times 10^3\$/\mathrm{year}\right) = \mathrm{OC} + \mathrm{FCI/PP}$$

PP represents the Payback Period, set at 3 years; OC denotes operating cost, includes steam costs, and entrainer supplement costs. Cooling water costs, significantly lower than steam costs, are neglected. The utility price, namely low-pressure steam ($7.78/GJ, 6 bar, 433 K), is referenced from the section 5.4 in Luyben's book [42]. FCI, namely capital investment, involves columns, and heat exchangers including condensers and reboilers. Small units such as pipes, valves, reflux tanks, pumps are disregarded because of their relative low cost. Diameters of the two columns are estimated using the "Tray Sizing" function in Aspen Plus. The overall tray efficiency for each column is assumed at 50 % for practice height design. Total heat transfer coefficients for the condenser and reboiler are assumed at 0.568 kW/(K·$m^2$) and 0.852 kW/(K·$m^2$), respectively. Detailed calculation formulas related to FCI can be found in SI.

$CO_2$ emissions are an important part of environmental impact evaluation [43]. Utility devices in distillation units are major contributors to $CO_2$ emissions [44]. Hence, $CO_2$ emissions warrant significant attention. Relevant formulas and calculation methods are derived from Gadalla

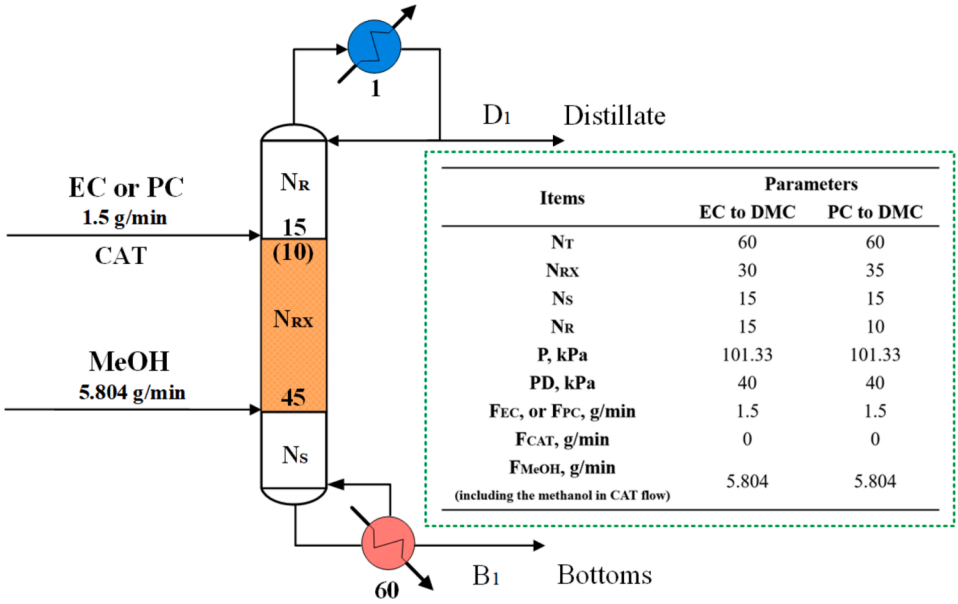


| Items | Parameters | |
|---|---|---|
| | EC to DMC | PC to DMC |
| $N_T$ | 60 | 60 |
| $N_{RX}$ | 30 | 35 |
| $N_S$ | 15 | 15 |
| $N_R$ | 15 | 10 |
| P, kPa | 101.33 | 101.33 |
| PD, kPa | 40 | 40 |
| $F_{EC}$, or $F_{PC}$, g/min | 1.5 | 1.5 |
| $F_{CAT}$, g/min | 0 | 0 |
| $F_{MeOH}$, g/min (including the methanol in CAT flow) | 5.804 | 5.804 |

**Fig. 5.** Process flowsheet and initial specification of the laboratory RD model.

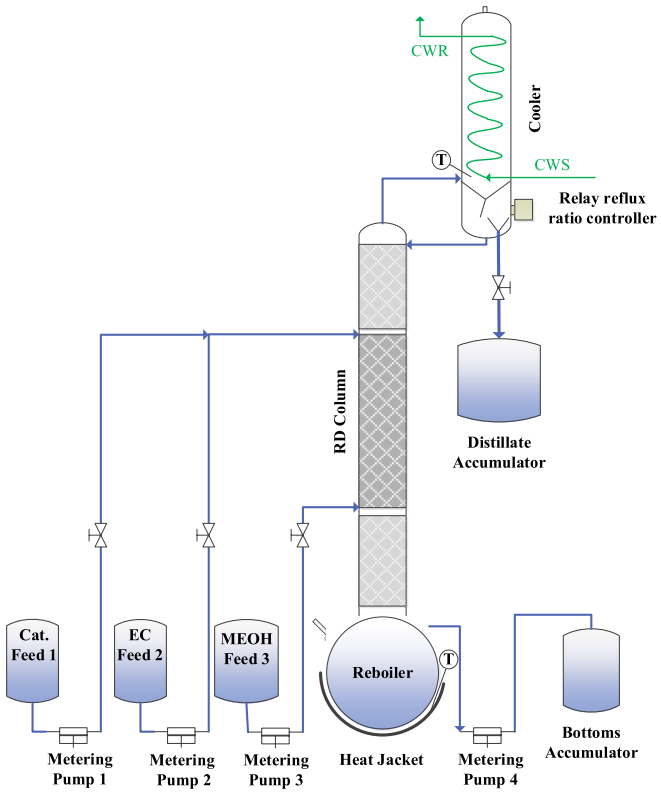


**Fig. 6.** Sketch of laboratory reactive distillation column setup.

[44], Yang [45] and Shen [43], as follows:

$$CO_2 \text{ emissions} = \left(\frac{Q_{fuel}}{NHV}\right)\left(\frac{C\%}{100}\right)\alpha$$

where $Q_{fuel}$ (kJ/h) is the total heat of the heating device in the RD process. The coefficient α is 3.67 in equation, and the NHV (kJ/kg) represents the net heating value of a fuel containing a carbon content of C%. The calculation formula for $Q_{fuel}$ and additional detailed parameters are available in Table S1 (SI).

### 4.2. Scaled-up EC RD process

According to the simulation practice and the interaction between reaction and distillation, the specifications of distillate and bottoms are set at 0.27 wt/wt DMC and $5 \times 10^{-7}$ wt/wt DMC respectively.

#### 4.2.1. Optimizing parameters

***Effect of Pressure.*** The base pressure is set as 1 bar. Table 7 gives the results for the energy consumption, products losses, and bottoms flowrate over a quite narrow pressure range due to the kinetics data obtained at atmospheric pressure. An extremely high sensitivity to pressure is clearly revealed. A quite significant increase (+43.5 %) in energy consumption should be required with a small reduction in pressure from 1 to 0.8 bar. The bottoms flowrate and the small products losses (DMC, EG) are almost constant with pressure variations, indicating the slight effluences on the downstream separation. Hence, the optimum operating pressure is 1 bar.

This phenomenon can be explained as follows. In conventional distillation, column pressure only affects the VLE. However, in reactive distillation, pressure affects both chemical kinetics and VLE. The backward specific reaction rate increases more quickly than the forward specific reaction rate with increasing temperature due to its larger activation energy, and thus decreases the chemical equilibrium constant (Fig. 10). Increasing pressure entirely rises the temperature profile within the column (Fig. 11), and thus entirely and slightly reduces the chemical equilibrium constant $K_{EQ}$ (Fig. 12). Fortunately, for pressures ranged from 1.1 to 0.8 bar, staged concentrations almost achieve chemical equilibrium because the $K_{cs}$ based on staged concentration almost approaches to the theoretical $K_c$ as calculated according to the calibrated kinetics by us at corresponding staged temperature (Fig. 12). This suggests that the reaction does not dominates the RD column, but the distillation separation determines the status of the RD column.

In the rectifying section, an operating pressure of 1.0 bar provides a DMC composition of 0.26 wt/wt escaping from the top of the reactive section (Fig. 13), which is close to the distillate specification of 0.27 wt/wt DMC and much higher than the operating pressure of < 1.0 bar does. This suggests that the reflux ratio increases as the operating pressure decreases from 1.0 to 0.7 bar. In the stripping section, an operating pressure of 1.0 bar provides the EG composition of 0.133 wt/wt escaping from the bottom of the reactive section (Fig. 13), which is close to the bottom's purity of 0.372 wt/wt EG and much higher than the operating pressure of < 1.0 bar does. This suggests that the boilup ratio increases as the operating pressure decreases from 1.0 to 0.7 bar. At an operating pressure of 1.1 bar, the azeotropic composition rising to 0.71/0.29 wt/wt MeOH/DMC owns a lower DMC composition compared to 0.69/0.31 wt/wt MeOH/DMC at 1 bar. Thus, much DMC should escape from the bottoms once the distillate specification is still set at 0.27 wt/wt DMC. Therefore, operating pressure of 1 bar is the optimum that offers the minimized energy consumption.

***Effect of Number of Reactive Trays.*** Table 8 gives results over a range of values of the number of reactive trays while keeping the numbers of stripping and rectifying trays constant at a pressure of 1 bar. There is an optimum reactive tray number of 30 minimizing the energy consumption. Abnormally, adding more reactive trays from the base 30 to 35 brings about a significant increase (+18.7 %) in energy consumption, whereas decreasing the reactive trays below 30 makes the bottoms composition violated. Products losses and the bottoms flowrate are almost constant and insensitive to the variations of the reactive trays from 30 to 35.

The explanation of the counterintuitive result can be referred from the composition profiles show in Figure S2 and S3 (SI). With few reactive trays, a lot of boilup ratio is required to keep the reactant EC from dropping down the column while a lot of reflux ratio is required to keep the reactant MeOH rising to the distillate. The situation is just the reverse with a large number of reactive trays. The concentrations of the reactants at the ends of the column where they are fed become large because much of the other reactant has been consumed on the many trays in the reactive zone before it reaches the opposite end. There is little EC arriving near the bottom of the reactive zone, and thus the concentration of MeOH is large near where it is fed. The concentration of EC is large near where it is fed since there is little MeOH arriving near the top of the reactive zone. These high concentrations near the feeding trays require more vapor boilup and reflux to keep EC from escaping out of the top and MeOH dropping out of the bottoms of the column.

***Effect of Number of Stripping and Rectifying Trays.*** As expected,

**Table 5**
Parameters for the Laboratory RD Column.

| Items | Parameters |
|---|---|
| Operation pressure | Atmospheric pressure |
| Reflux ratio | Adjusted with Elec-relay reflux ratio controller |
| Overhead temperature, $T_T$ | Monitored with temperature indictor |
| Bottoms temperature, $T_B$ | Monitored with thermometer |
| Heating jacket temperature | Controlled with temperature indictor |
| location of EC (catalyst) feeding inlet | ~530 mm from the top packing |
| location of MeOH feeding inlet | ~1530 mm from the top packing |
| Rectifying section | 530 mm (2 mm × 2 mm Dixon) |
| Reactive section | 1000 mm (2 mm × 2 mm Dixon) |
| Stripping section | 400 mm (2 mm × 2 mm Dixon) |

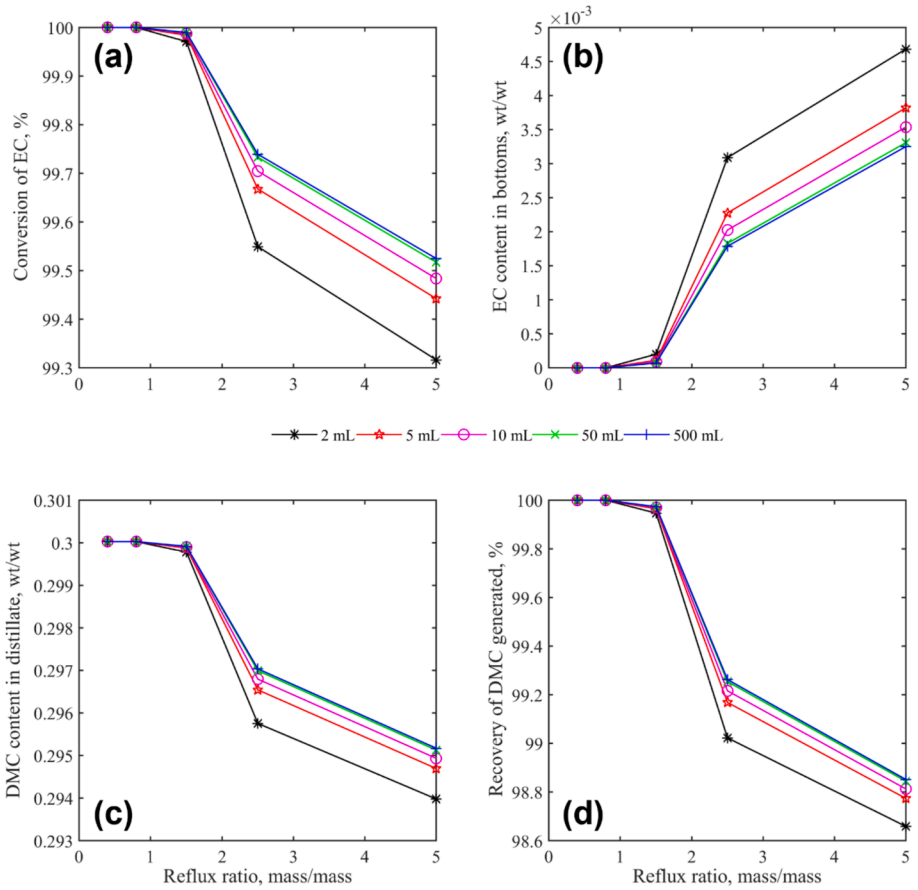


**Fig. 7.** The influence of reflux ratio with various liquid holdup on (a) EC conversion, (b) EC content in bottoms, (c) DMC content in distillate, and (d) recovery of DMC generated at overhead pressure of 101.33 kPa and column pressure drop of 40 kPa.

more stripping trays would make the fractionation easier and require lower boilup ratio, and therefore the energy consumption is reduced with increasing stripping trays as shown in Table 9. However, as the stripping trays increases exceeding 15, the effects of stripping trays on the energy consumption, products losses, and the bottoms flowrate becomes rather insensitive. Thus, the optimized stripping tray is 15. The effects of rectifying trays are quite sensitive with the variations from the base 15 such that the DMC specification in the bottoms cannot be achieved with the rectifying trays less or more than 15, as demonstrated in Table 10. This is a surprising that remains a mysterious.

***Effect of Holdup on Reactive Trays.*** Increasing holdup on reactive trays improves performance, as almost in all the ideal cases revealed by Luyben and Yu [40]. However, the liquid holdup on the reactive trays cannot be infinitely large but should be limited by column diameter mainly determined by boilup rate. Table 11 shows this trend that decreasing the reactive tray holdup from the base 13.4 to 1 $m^3$ results in a slight increase (+4.8 %) in energy consumption with almost no effects on products losses and bottoms flowrate. However, as the liquid holdup decreases to 0.5 $m^3$, the bottoms specification cannot be achieved. Thus, the optimized holdup should be 1 $m^3$.

To explain the phenomenon above, it is calculated that at various holdups exceeding 1 $m^3$, the staged concentrations almost achieve chemical equilibrium because the $K_{cs}$ based on staged concentration almost approaches to the theoretical $K_c$ as calculated according to the calibrated kinetics by us at corresponding staged temperature (Fig. 14). This suggests that the reaction does not dominates the RD column, but the distillation separation determines the status of the RD column. However, as the holdup decreases from 1 to 0.5 $m^3$, the $K_{cs}$ gradually drifts away from the $K_c$. Further decreasing the holdup to 0.1 $m^3$, the $K_{cs}$ keeps away from the $K_c$ curve, especially at the lower part of the reactive section. This implies that as the holdup decreases to lower than 1 $m^3$, the reaction, instead of distillation separation, is raised to dominate the status of the RD column because of the lowering extent of reaction on reactive trays. In this case, the low holdup does not offer sufficient liquid volume to make the reaction approaching the chemical equilibrium.

#### 4.2.2. *Optimized EC RD design*

The optimized EC RD design is as listed in Table 11, corresponding to the case 1 $m^3$ holdup, and shown in the section 4.4. This design differs somewhat from the EC RD column reported by Fang et al. [24].

(1) **Higher reaction rate:** The kinetics calibrated by us exhibits a significantly higher reaction rate, with a unit of $kmol \cdot m^{-3} \cdot s^{-1}$ rather than $kmol \cdot m^{-3} \cdot min^{-1}$. Thus, the time required to reach the reaction equilibrium is only ~2 min.
(2) **High EC conversion:** The EC conversion achieves > 99.95 % at a reasonably low holdup of 1 $m^3$ avoiding the use of CSTR trains, in contrast to the quite high holdup reported in the laboratory experiment by Fang et al. [24].

### 4.3. *Scaled-up PC RD process*

According to the simulation practice and the interaction between reaction and distillation, the specifications of distillate and bottoms for PC RD are roughly set at 0.27 wt/wt DMC and 1 × $10^{-5}$ wt/wt DMC respectively.

#### 4.3.1. *Optimizing parameters*

***Effect of Pressure.*** Table 12 clearly demonstrates the extremely high sensitivity of the process to pressure. In contrast to the EC RD, a quite

**Table 6**
Comparisons of the simulated and experimental results at various flowrates[d].

| | | Flowrate, g/min | | | | Temperature, °C | Compositions at Distillate or Bottoms, wt/wt | | | | | Conversion, % | Selectivity, % | | Mass Balance, % | |
|---|---|---|---|---|---|---|---|---|---|---|---|---|---|---|---|---|
| | | Cat | EC | MEOH | B | D | Top/Reboiler | | MEOH | DMC | EG | EC | others | EC | DMC | EG | Total | DMC |
| 1 | SIM | 0.469 | 0.572 | 2.334 | 1.161 | 2.214 | 64.0/72.5 | D | 0.737 | 0.263 | Trace | Trace | / | **99.9** | / | / | **0** | **0** |
| | | | | | | | | B | 0.644 | 2.0E-4 | 0.346 | 6.0E-4 | / | | | | | |
| | EXP | 0.469 | 0.572 | 2.334 | 1.153 | 2.214 | 63.5–64/ | D | 0.727 | 0.268 | 0.0002 | 0.0001 | 0 | **99.96** | 102 | 93 | **−0.22** | **1.53** |
| | | | | | | | 73.1–73.6 | B | 0.616 | 0.002 | 0.323 | 0.0006 | 0.0019 | | | | | |
| 2 | SIM | 0.75 | 0.915 | 3.537 | 1.742 | 3.46 | 64.0/72.5 | D | 0.729 | 0.271 | Trace | Trace | / | **99.98** | / | / | **0** | **0** |
| | | | | | | | | B | 0.630 | 0.370 | 7.5E-5 | 0.002 | / | | | | | |
| | EXP | 0.750 | 1.034 | 3.537 | 1.988 | 3.460 | 63.7–64/ | D | 0.689 | 0.313 | 0.0005 | 0.0001 | 0.0001 | **99.95** | 103 | 91 | **2.38** | **2.84** |
| | | | | | | | 72.8–73.6 | B | 0.620 | 0.002 | 0.332 | 0.0007 | 0.002 | | | | | |
| 3 | SIM | 0.900 | 1.138 | 4.388 | 2.207 | 4.219 | 64.0/72.5 | D | 0.726 | 0.274 | Trace | 0 | / | **99.8** | / | / | **0** | **0** |
| | | | | | | | | B | 0.634 | 0.002 | 0.363 | 8.5E-4 | / | | | | | |
| | EXP | 0.900 | 1.138 | 4.388 | 2.506 | 4.219 | 63.7–64/ | D | 0.710 | 0.290 | 0.0005 | 0.0001 | 0 | **99.99** | 101 | 101 | **3.79** | **0.64** |
| | | | | | | | 72.8–73.6 | B | 0.634 | 0.0003 | 0.344 | 0.0001 | 0.0012 | | | | | |
| 4 | SIM | 0.956 | 1.252 | 4.709 | 2.517 | 4.400 | 64.0/72.5 | D | 0.719 | 0.281 | Trace | Trace | / | **99.6** | / | / | **0** | **0** |
| | | | | | | | | B | 0.620 | 0.005 | 0.373 | 0.002 | / | | | | | |
| | EXP | 0.956 | 1.252 | 4.709 | 2.732 | 4.280 | 63.7–64/ | D | 0.689 | 0.298 | 0.0006 | 0.0001 | 0.0001 | **99.99** | 99.6 | 98.4 | **1.38** | **−0.44** |
| | | | | | | | 72.8–73.6 | B | 0.643 | 0.0004 | 0.317 | 0.0001 | 0.001 | | | | | |

[d] : Each experimental point is obtained for ~ 8h after the parameters are varied and kept steady state more than 2 h via separately weighing accumulation of distillate and bottoms and mass reduction of MEOH, EC, and CAT tank by using electronic balance. Metering pumps are also used for mass flow measurement and indication.

significant reduction (−51.9 %) from 25.66 to 12.34 MW in energy consumption is achieved with reducing pressure from 1 to 0.8 bar, whereas surprisingly energy consumption significantly increases with increasing pressure from 1 to 1.1 bar. Meanwhile, for all the cases, complete conversion of PC (>99.98 %) can be achieved, with constant bottoms flowrate and quite small products losses. Considering the limitation of the kinetics experiment of by Zhang at al.[23], further reducing pressure could bring about misleading simulated result. Hence, an operating pressure of 0.8 bar is the optimum, achievable by using a vacuum pump.

Fig. 15 Shows that the rate constants $k_{1+}$ almost keep constant and $k_{2-}$ increases with increasing temperature ranging from 327 to 347 K, and thus decreases the chemical equilibrium constant $K_c$. The chemical equilibrium constant by using the staged liquid molarity ($K_{cs}$) in contrast to that by using the Zhang's [23] kinetics ($K_c$) has been calculated as shown in Fig. 16 with the temperature profile detailed in Figure S4 (SI). It is revealed that operating pressure has an essentially influence on the PC RD column caused by the various kinetics rates induced by pressure variation. As the pressure increases, the $K_c$ profile overall and gradually decreases, while the $K_{cs}$ also overall and gradually decreases, especially with increasing pressure from 0.8 to 1.0 bar, but $K_{cs}$ substantially decreases with increasing pressure from 1.0 to 1.1 bar. Thus, the $K_{cs}$ profile becomes near the $K_c$ profile as increasing pressure from 0.8 to 1.0 bar, but becomes farther away from the $K_c$ profile as increasing pressure from 1.0 to 1.1 bar. On the other hand, the stripping section could control the PC RD column because the high concentration of methanol (>0.88 wt/wt) has to be stripped to a moderate composition (~0.61 wt/wt) which requires a large boilup ratio, as the composition profile as shown in Figure S5 (SI). Meanwhile, reducing pressure decreases the azeotropic MeOH composition, distances the T-x and T-y curves, and thus facilitates the separation; Hence, the required reflux ratio is substantially reduced.

***Effect of Number of Reactive Trays.*** As revealed in Table 13, at the pressure of 0.8 bar, adding more reactive trays from 35 to 45 brings about a marginal reduction (−9.8 %) in energy consumption with fixed stripping and rectifying trays, whereas reducing reactive trays from 35 to 30 significantly rises energy consumption from 12.34 to 13.46 MW (+9%). For all the cases, high conversion of PC is achieved at > 99.97 %, with the products losses and bottoms kept nearly constant. In all, the optimized reactive trays can be still at 35.

***Effect of Number of Stripping and Rectifying Trays.*** Like the case of EC to DMC, Table 14 presents that the effects of stripping trays on the energy consumption, products losses, and the bottoms flowrate is rather insensitive, especially the stripping trays exceeding 15. Thus, the optimized stripping trays is 15. Energy consumption is also quite insensitive to the decreasing rectifying trays from the base 15 to 5, as demonstrated in Table 15. The underlining reason for this phenomenon can be also explained by using the temperature and composition profiles within the PC RD column. The rectifying trays is optimized and reduced to be 10. This is unsurprising that the separation of PC and MeOH-DMC azeotrope is quite easier because of the quite larger difference in boiling point of PC/MeOH than that of EG/MeOH.

***Effect of Holdup on Reactive Trays.*** Table 16 shows this trend that decreasing the reactive tray holdup from the base 47.6 to 10 $m^3$ increases energy consumption by 11.8 %, with the products losses and bottoms constant. However, as the holdup continuously decreases to 2 $m^3$, the energy consumption significantly increases and the conversion of PC becomes lower than 99 % due to the insufficient liquid holdup to achieve sufficient reaction extent on each tray. Thereafter, the PC conversion can be maximized at 98.6 % at the optimized reflux ratio of 1.8 with significantly increased energy consumption of 19.62 MW.

Further decreasing the holdup to 1 $m^3$, the PC conversion markedly declines to 94.58 % with a soaring energy consumption of 23.72 MW, indicating lots of the unreacted PC undesired escaping from the bottoms. The DMC specification of the distillate can be loosened to low values (0.25, 0.26 wt/wt) because low DMC formation rate at low holdup requires little DMC being distillated. Thus, at the holdup of 1 $m^3$, as shown

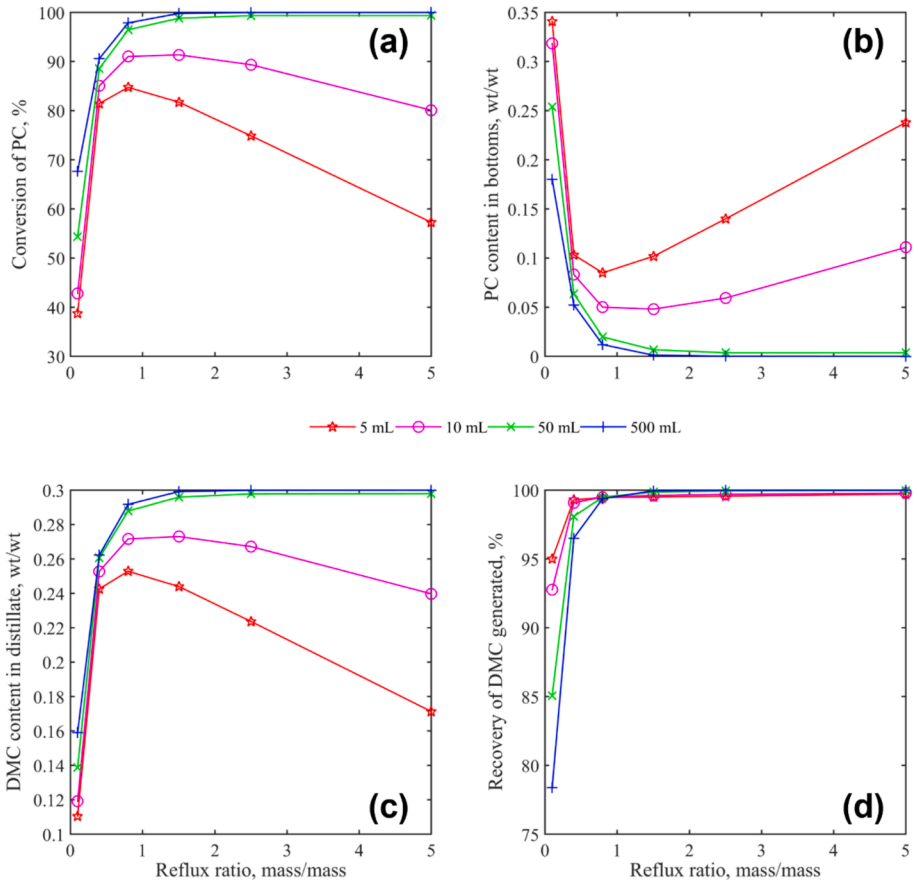


**Fig. 8.** The influence of reflux ratio with various liquid holdup 5, 10, 50, and 500 mL on (a) PC conversion, (b) PC content in bottoms, (c)DMC content in distillate, and (d)recovery of DMC generated at overhead pressure of 101.33 kPa and column pressure drop of 40 kPa.

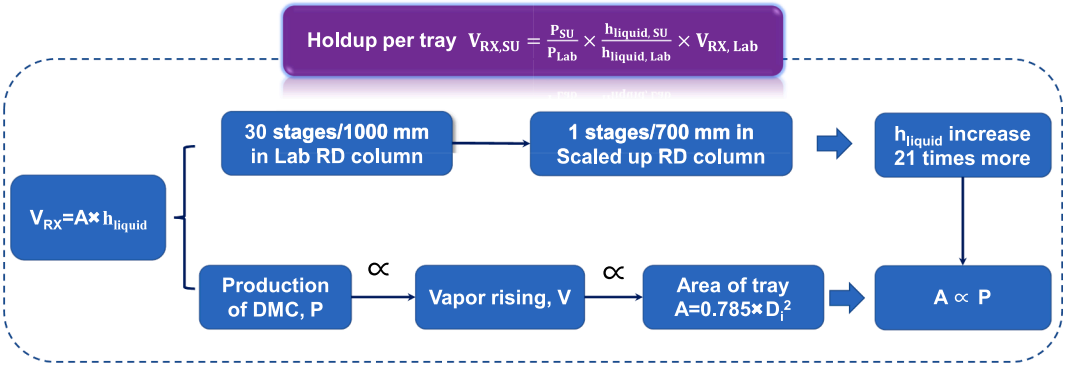


**Fig. 9.** Scaled-up times of holdup per tray estimated.

**Table 7**
Effect of Pressure of EC transesterification RD.

| Pressure (bar) | Reboiler Heat Input (MW) | Reflux Ratio (kg/kg) | Reboiler Ratio (kg/kg) | DMC in Bottoms (kg/h) | EG in Distillate (kg/h) | Bottoms (kg/h) |
|---|---|---|---|---|---|---|
| 1.1 | 9.12 | 0.35 | 2.53 | 44.93 | 3.82E-7 | 13943.66 |
| **1.0** | **7.75** | **0.17** | **2.12** | **0.01** | **1.19E-4** | **13914.90** |
| 0.9 | 9.62 | 0.45 | 2.60 | 0.01 | 1.01E-9 | 13914.90 |
| 0.8 | 11.12 | 0.68 | 2.98 | 0.01 | 1.96E-12 | 13914.90 |

Base design parameters: $N_T$=60, $N_{RX}$=30, $N_S$=15, $N_R$=15, $V_{RX}$=13.4 $m^3$.

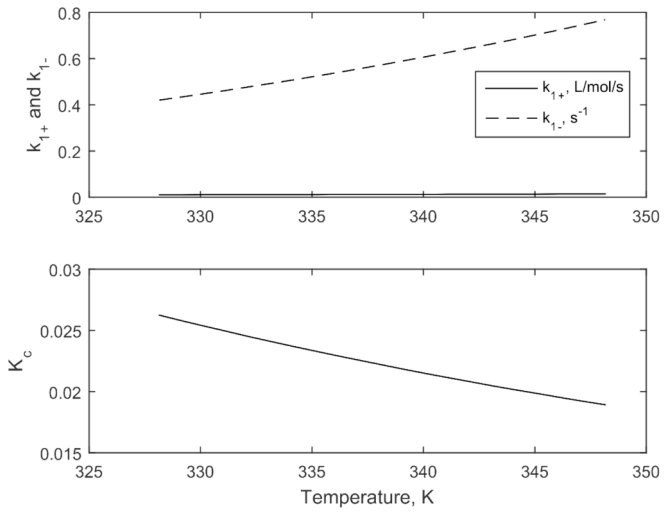


**Fig. 10.** Rate constants $k_{1+}$ and $k_{1-}$, and chemical equilibrium constant $K_c$ at various temperatures by using the calibrated kinetics.

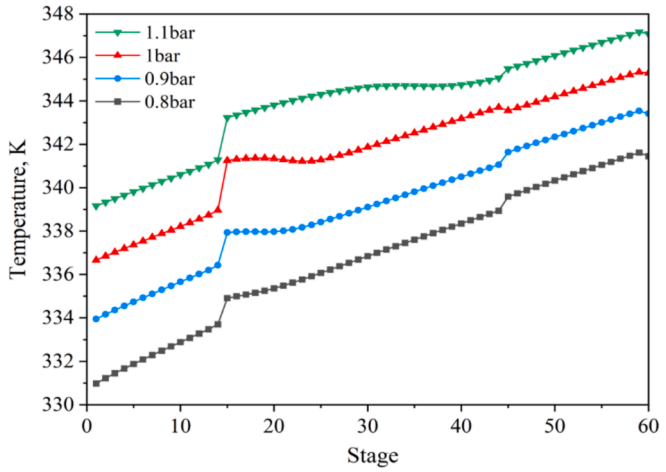


**Fig. 11.** Temperature profile within the reactive distillation column at various pressures.

in Fig. 17, for each DMC specification of 0.31, 0.3, 0.29, 0.28, 0.27, 0.26 and 0.25 wt/wt, there exists an optimum reflux ratio (RR) that achieves the highest PC conversion ($X_{PC}$). Connecting these highest points generates reaction-separation boundary, where achieves perfect matching of reaction and distillation and thus highest $X_{PC}$. The left region is defined as reaction-restricted region since the limited reaction in this region requires relatively large reflux ratio to reflow the overhead unreacted reactant within the column. In contrast, the right one is defined as separation-restricted region since the limited distillation rate in this region requires small reflux ratio to ensure timely removal of the low-boiling product generated.

Considered that the diameter of the column is calculated around 3.5 m at the holdup of 2 $m^3$, which requires around 208 mm liquid height on each tray that is somewhat too high in spite of its low bottoms PC content. There should existed a balance between the holdup and the bottoms PC content that offers both a decreased holdup and a low bottoms PC content. The "Flowsheeting Options/Design Specs" function is employed by varying the holdup to satisfy the bottoms PC content at 0.0056 wt/wt. Thus, the optimized holdup is reduced to 1.82 $m^3$.

Fig. 18 reveals the variations of the difference between chemical equilibrium constant $K_{cs}$ and the theoretical $K_c$ gradually enlarges as the holdups decreases from 46.7 to 10 $m^3$; Then the difference significantly enlarges with decreasing holdup from 10 to 2 $m^3$, at which the holdup becomes insufficient for the PC to DMC reaction, elucidating why the PC conversion markedly decreases. Further decreasing holdup from 2 to 1 $m^3$ also markedly enlarges the difference. Fortunately, reducing the DMC specification of the distillate at 0.25 wt/wt and properly increasing the PC composition in the bottoms at 0.0056 wt/wt make the difference ($K_{ck} - K_c$) profile like that of the holdup of 2 $m^3$. This adjustment alters the composition profile and promotes the reaction, which provide appropriate matching between the reaction and distillation processes.

#### 4.3.2. *Optimized PC RD design*

The optimized RD design, as listed in Table 16 related to the case of holdup of 1.82 $m^3$ and shown in Fig. 19**b**, is quite different from the PC RD column reported by Huang et al. [2]:

(1) **Reduced operating pressure:** The operating pressure is reduced to 0.8 bar, rather than 1.0133 bar used by Huang et al.[2]. this reduction both increases the azeotropic MeOH composition from 0.7 to 0.67 and facilitates the separation within the pinch zone.
(2) **Lower bottoms PC content:** The bottoms PC content is reduced to only 0.0056 wt/wt, significantly lower than 0.0144 wt/wt according to Huang et al. [2]. This reduction could avoid the complex hydrolysis process downstream and reduces capital investment cost.
(3) **High PC conversion:** The PC conversion achieves > 99 % at the expense of a quite higher holdup of 1.82 $m^3$ for producing ~60 ktpy of DMC, compared to a tray liquid holdup of 150–200 L for 17 ktpy of DMC according to Huang et al. [2].

### 4.4. *Economic and $CO_2$ emissions comparison*

Once the optimized designs of the RDs via the two DMC routes are obtained as shown in Fig. 19, it is interesting and insightful to make a comparison of the two DMC routes in terms of operating cost (OC), fixed capital investment cost (FCI), and total annual cost (TAC). It is clearly that the EC RD offers considerable reductions of 58.1 % in OC and 40.1 % in FCI compared with the PC RD, resulting a reduction of 53.2 % in TAC as shown in Fig. 20**a**. These economic data suggests that the route of EC to DMC is significantly superior to that of PC to DMC.

Under the global constraints of "carbon emission reduction" and "carbon neutrality", the energy consumption and carbon dioxide emissions should be seriously compared under the global constraints of "carbon emission reduction" and "carbon neutrality". As shown in Fig. 20**b**, the EC RD process has an energy consumption of only 29.3 GJ/h corresponding to 1.9 t LPS/t DMC, which is around 57.8 % lower than the consumption (69.6 GJ/h) of the PC RD corresponding to 4.5 t LPS/t DMC. Similarly, the EC RD process (1.9 t/h) offers considerable $CO_2$ emissions reduction by around 57 % compared with the PC RD process does (4.4 t/h). Hence the EC to DMC is much more energy-efficient and low-carbon route than that of PC to DMC route.

## 5. Conclusions

To quantitively assess the two RD processes, EC to DMC and PC to DMC, and well elucidate the interplay between reaction and separation, we conducted comprehensive comparison in terms of kinetic insights, laboratory RD modelling and analyses, and scaled-up RD processes involving operating cost, total annual cost, energy consumption and $CO_2$ emissions.

For the EC to DMC RD process, with the calibrated kinetics by us, the EC conversion achieves > 99.95 % at a reasonable low holdup of 1 $m^3$, avoiding the use of CSTR trains, as opposed to the laboratory experiment by Fang et al.[24]. For the PC to DMC RD, the operating pressure was reduced to 0.8 bar, different with 1.0133 bar by Huang et al.[2], which eases the pinch-zone separation. The bottoms PC content is reduced to only 0.0056 wt/wt, avoiding the complex hydrolysis process downstream. The PC conversion achieves > 99 % at the expense of a higher

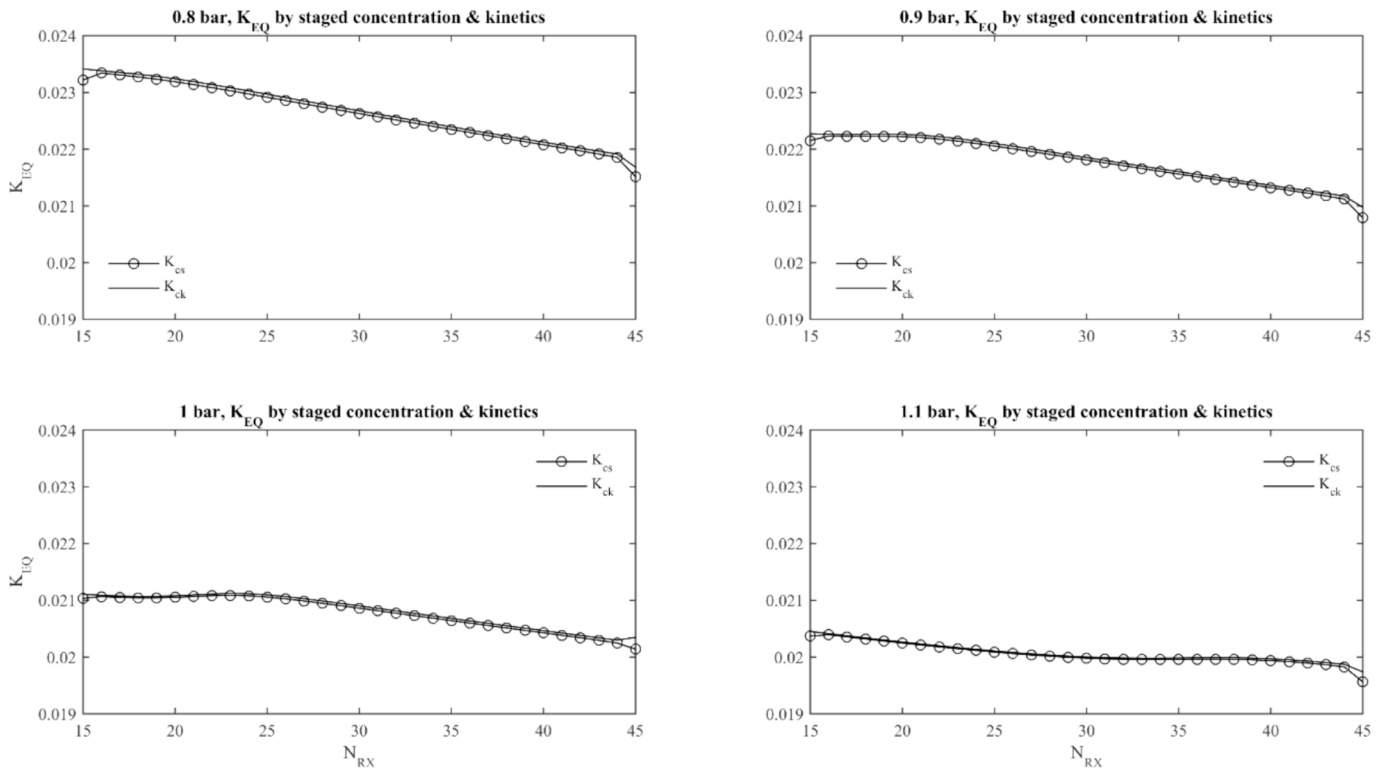


**Fig. 12.** Chemical equilibrium constant $K_{cs}$ based on staged concentration compared to the theoretical $K_c$ according to our calibrated kinetics along the reactive trays at various operating pressures.

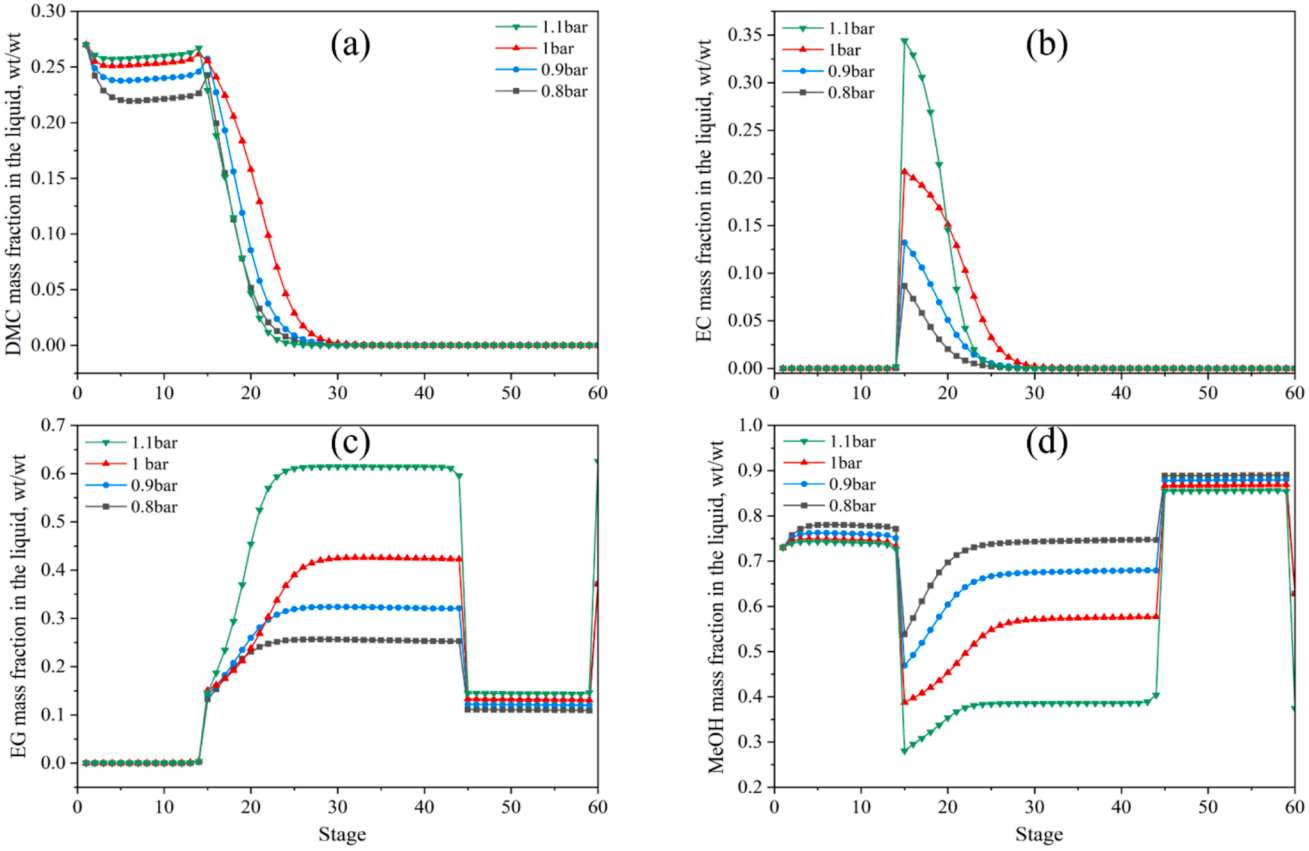


**Fig. 13.** Composition profile within the reactive distillation column at various pressures: mass fraction of (a) DMC, (b) EC, (c) EG and (d) MeOH in the liquid.

**Table 8**
Effect of Number of Reactive Trays of EC transesterification RD[a].

| $N_{RX}$ | $N_T$ | Reboiler Heat Input (MW) | Reflux ratio (kg/kg) | Boilup ratio (kg/kg) | DMC in Bottoms (kg/h) | EG in Distillate (kg/h) | Bottoms (kg/h) |
|---|---|---|---|---|---|---|---|
| 35 | 65 | 9.20 | 0.38 | 2.52 | 6.96E-3 | 3.74E-08 | 13914.89 |
| 32 | 62 | 8.74 | 0.31 | 2.39 | 6.96E-03 | 2.32E-07 | 13914.89 |
| **30** | **60** | **7.75** | **0.17** | **2.12** | **6.96E-03** | **1.19E-04** | **13914.90** |
| 28[b] | 58 | 8.69 | 0.3 | 2.38 | 0.056 | 3.06E-07 | 13915.15 |

[a] : Other design parameters: $N_S$=15, $N_R$=15, $V_{RX}$=13.4 $m^3$, P=1 bar, dP=0.4 bar
[b] : The DMC specification in the bottoms cannot be achieved.

**Table 9**
Effect of Number of Stripping Trays of EC transesterification RD[a].

| $N_S$ | $N_T$ | Reboiler Heat Input (MW) | Reflux ratio (kg/kg) | Boilup ratio (kg/kg) | DMC in Bottoms (kg/h) | EG in Distillate (kg/h) | Bottoms (kg/h) |
|---|---|---|---|---|---|---|---|
| 20 | 65 | 7.62 | 0.15 | 2.08 | 6.96E-03 | 3.82E-04 | 13914.90 |
| 17 | 62 | 7.69 | 0.16 | 2.10 | 6.96E-03 | 2.07E-04 | 13914.90 |
| **15** | **60** | **7.75** | **0.17** | **2.12** | **6.96E-03** | **1.19E-04** | **13914.90** |
| 13 | 58 | 7.90 | 0.18 | 2.15 | 6.96E-03 | 5.04E-05 | 13914.90 |

[a] : Other design parameters: $N_{RX}$=30, $N_R$=15, $V_{RX}$=13.4 $m^3$, P=1 bar, dP=0.4 bar.

**Table 10**
Effect of Number of Rectifying Trays of EC transesterification RD[a].

| $N_R$ | $N_T$ | Reboiler Heat Input (MW) | Reflux ratio (kg/kg) | Boilup ratio (kg/kg) | DMC in Bottoms (kg/h) | EG in Distillate (kg/h) | Bottoms (kg/h) |
|---|---|---|---|---|---|---|---|
| 20[b] | 65 | 8.01 | 0.2 | 2.19 | 0.016 | 1.04E-07 | 13914.90 |
| 17[b] | 62 | 8.01 | 0.2 | 2.19 | 7.45E-03 | 2.05E-06 | 13914.90 |
| **15** | **60** | **7.75** | **0.17** | **2.12** | **6.96E-03** | **1.19E-04** | **13914.90** |
| 13[b] | 58 | 8.73 | 0.3 | 2.40 | 11.7 | 4.87E-10 | 13966.69 |

[a] : Other design parameters: $N_{RX}$=30, $N_S$=15, $V_{RX}$=13.4 $m^3$, P=1 bar, dP=0.4 bar
[b] : The DMC specification in the bottoms cannot be achieved.

**Table 11**
Effect of Holdup on Reactive Trays of EC transesterification RD[a].

| $V_{RX}$ ($m^3$) | Reboiler Heat Input (MW) | Reflux ratio (kg/kg) | Boilup ratio (kg/kg) | DMC in Bottoms (kg/h) | EG in Distillate (kg/h) | Bottoms (kg/h) |
|---|---|---|---|---|---|---|
| 13.4 | 7.75 | 0.17 | 2.12 | 0.01 | 1.19E-04 | 13914.90 |
| 5.0 | 8.29 | 0.25 | 2.27 | 7.00E-3 | 2.30E-6 | 13914.90 |
| **1.0** | **8.12** | **0.22** | **2.22** | **7.00E-3** | **6.86E-6** | **13914.90** |
| 0.5[b] | 8.01 | 0.2 | 2.19 | 0.01 | 0 | 13914.90 |

[a] : Other design parameters: $N_{RX}$=30, $N_S$=15, $N_R$=15, P=1 bar, dP=0.4 bar
[b] : The DMC specification in the bottoms cannot be achieved.

holdup of 1.82 $m^3$ for producing ~60 ktpy of DMC, compared to a tray liquid holdup of 150–200 L for 17 ktpy DMC by Huang et al [2]. The interplay and control factors between reaction and separation are elucidated and clarified via investigating variations of actual chemical equilibrium constant profile compared with theoretical value profiles along the reactive section at various pressures, liquid holdups, etc. The comparison results reveal that the optimized EC RD process offers almost 50 % reductions in both economy and $CO_2$ emissions compared to the PC RD process. Hence the EC to DMC RD process is much more energy-efficient and low-carbon route than the PC to DMC RD process. This work facilitates the carbon neutrality and provides a useful guide for quantitatively selecting and retrofitting the two processes.

Considered the interplay between reaction and separation, dynamics control of the process is necessarily studied for ensuring the economic and $CO_2$ emissions advantage. Meanwhile, research and development of heterogeneous catalyst with sufficient reactivity over the traditional homogeneous catalyst is necessary for avoiding the tricky separation of catalyst.

## Declaration of competing interest

The authors declare that they have no known competing financial interests or personal relationships that could have appeared to influence the work reported in this paper.

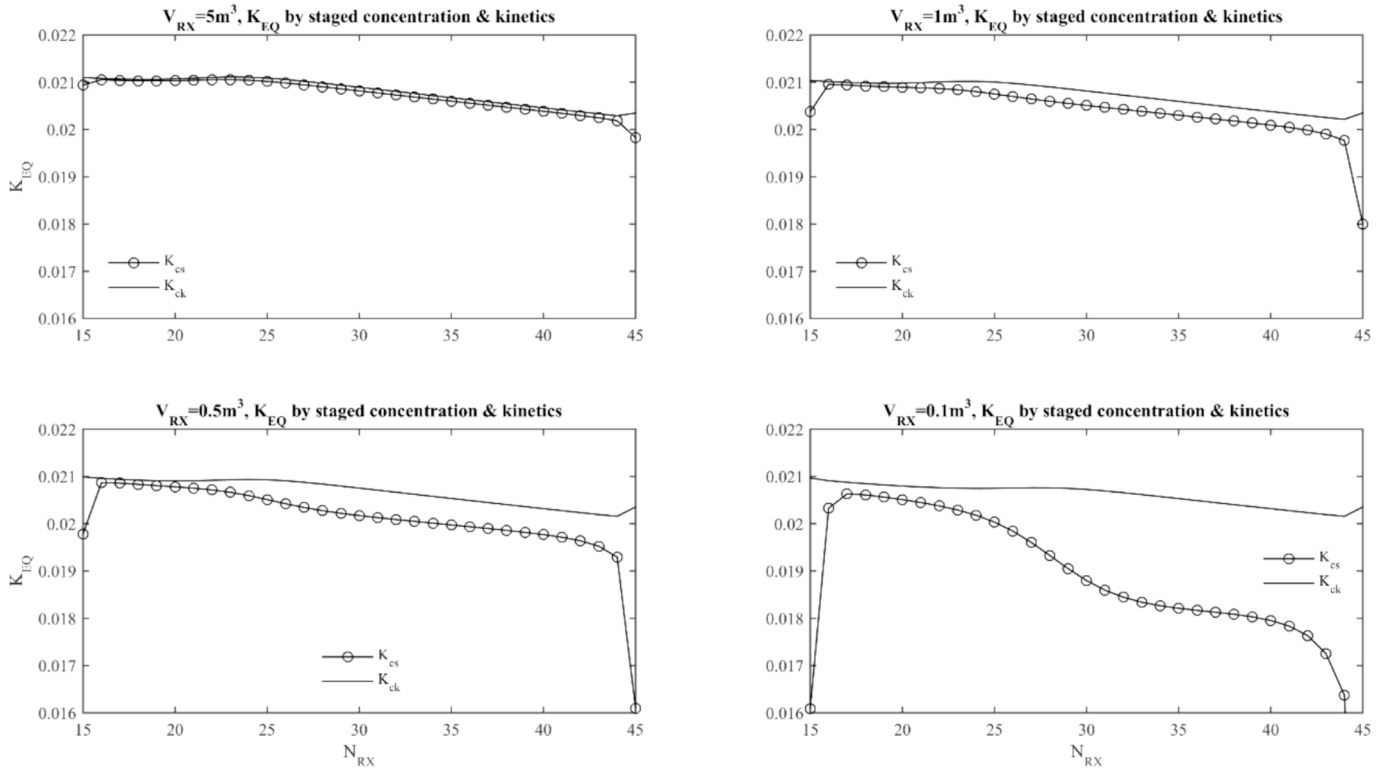


**Fig. 14.** Chemical equilibrium constant $K_{cs}$ based on staged concentration compared to the theoretical $K_c$ according to our calibrated kinetics along the reactive trays at various holdups.

**Table 12**
Effect of Pressure of PC transesterification RD[a].

| Pressure (bar) | Reboiler Heat Input (MW) | Reflux ratio (kg/kg) | Boilup ratio (kg/kg) | DMC in Bottoms (kg/h) | PG in Distillate (kg/h) | Bottoms (kg/h) | $X_{PC}$ (%) |
|---|---|---|---|---|---|---|---|
| 1.1 | 80.56 | 11.16 | 23.90 | 0.15 | 0 | 14825.00 | 99.99 |
| 1.0 | 25.66 | 2.71 | 7.59 | 0.15 | 0 | 14824.80 | 99.99 |
| 0.9 | 16.15 | 1.26 | 4.76 | 0.15 | 0 | 14825.50 | 99.99 |
| **0.8** | **12.34** | **0.69** | **3.62** | **0.15** | **0** | **14827.12** | **99.98** |

[a] : Base design parameters: $N_T$=60, $N_{RX}$=35, $N_S$=15, $N_R$=10, $V_{RX}$=47.6 $m^3$.

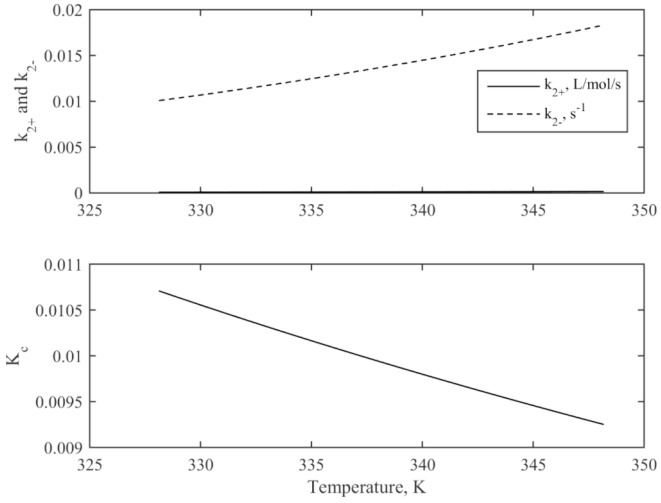


**Fig. 15.** Rate constants $k_{2+}$ and $k_{2-}$, and chemical equilibrium constant $K_c$ at various temperatures by using kinetics from Zhang et al. [23].

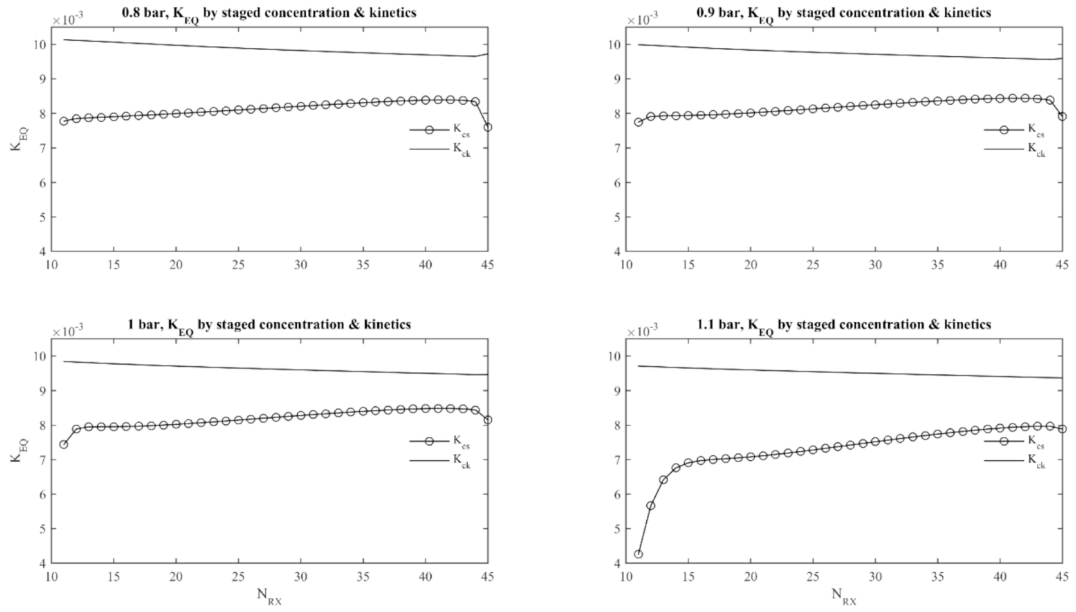


**Fig. 16.** Chemical equilibrium constant based on staged concentration $K_{cs}$ compared to the theoretical $K_c$ according to the Zhang's kinetics [23] along the reactive trays at various operating pressures.

**Table 13**
Effect of Number of Reactive Trays of PC transesterification RD[a].

| $N_{RX}$ | $N_T$ | Reboiler Heat Input (MW) | Reflux ratio(kg/kg) | Boilup ratio(kg/kg) | DMC in Bottoms(kg/h) | PG in Distillate(kg/h) | Bottoms(kg/h) | $X_{PC}$(%) |
|---|---|---|---|---|---|---|---|---|
| 45 | 70 | 11.13 | 0.51 | 3.27 | 0.15 | 0 | 14825.86 | 99.98 |
| 40 | 65 | 11.62 | 0.58 | 3.41 | 0.15 | 0 | 14826.35 | 99.98 |
| **35** | **60** | **12.34** | **0.69** | **3.62** | **0.15** | **0** | **14827.12** | **99.98** |
| 30 | 55 | 13.46 | 0.85 | 3.95 | 0.15 | 0 | 14828.44 | 99.97 |

[a] : Other design parameters: $N_S$=15, $N_R$=10, $V_{RX}$=47.6 $m^3$, P=0.8 bar, dP=0.4 bar.

**Table 14**
Effect of Number of Stripping Trays of PC transesterification RD[a].

| $N_S$ | $N_T$ | Reboiler Heat Input (MW) | Reflux ratio(kg/kg) | Boilup ratio(kg/kg) | DMC in Bottoms(kg/h) | PG in Distillate(kg/h) | Bottoms(kg/h) | $X_{PC}$(%) |
|---|---|---|---|---|---|---|---|---|
| 20 | 65 | 11.80 | 0.61 | 3.47 | 0.15 | 0 | 14829.96 | 99.97 |
| **15** | **60** | **12.34** | **0.69** | **3.62** | **0.15** | **0** | **14827.12** | **99.98** |
| 10 | 55 | 13.09 | 0.80 | 3.85 | 0.15 | 0 | 14824.99 | 99.99 |

[a] : Other design parameters: $N_{RX}$=35, $N_R$=10, $V_{RX}$=47.6 $m^3$, P=0.8 bar, dP=0.4 bar.

**Table 15**
Effect of Number of Rectifying Trays of PC transesterification RD[a].

| $N_R$ | $N_T$ | Reboiler Heat Input (MW) | Reflux ratio(kg/kg) | Boilup ratio(kg/kg) | DMC in Bottoms(kg/h) | PG in Distillate(kg/h) | Bottoms(kg/h) | $X_{PC}$(%) |
|---|---|---|---|---|---|---|---|---|
| 15 | 65 | 12.79 | 0.75 | 3.76 | 0.15 | 0 | 14827.30 | 99.98 |
| **10** | **60** | **12.34** | **0.69** | **3.62** | **0.15** | **0** | **14827.12** | **99.98** |
| 5 | 50 | 12.89 | 0.72 | 3.69 | 0.15 | 0 | 14824.92 | 99.99 |

[a] : Other design parameters: $N_{RX}$=35, $N_S$=15, $V_{RX}$=47.6 $m^3$, P=0.8 bar, dP=0.4 bar.

**Table 16**
Effect of Holdup on Reactive Trays of PC transesterification RD[a].

| $V_{RX}$ ($m^3$) | Reboiler Heat Input (MW) | Reflux ratio (kg/kg) | Boilup ratio (kg/kg) | DMC in Bottoms(kg/h) | PG in Distillate(kg/h) | Bottoms(kg/h) | $X_{PC}$(%) |
|---|---|---|---|---|---|---|---|
| 47.6 | 12.34 | 0.69 | 3.62 | 0.15 | 0 | 14827.12 | 99.98 |
| 20 | 12.82 | 0.76 | 3.76 | 0.15 | 0 | 14828.40 | 99.975 |
| 10 | 13.79 | 0.90 | 4.05 | 0.15 | 0 | 14831.10 | 99.965 |
| 2 | 19.62 | 1.8 | 5.59 | 1.05 | 0 | 15208.70 | 98.6 |
| 1.82[b] | 19.34 | 1.5 | 6.86 | 18.25 | 0 | 12912.2 | 99.15 |
| 1[c] | 22.72 | 2.5 | 5.69 | 192.05 | 0 | 17048.10 | 94.58 |

[a] : Other design parameters: $N_{RX}$=35, $N_S$=15, $N_R$=10, P=0.8 bar, dP=0.4 bar, $V_{RX}$ is varied
[b] : the optimized holdup with the DMC specification of the distillate reduced at 0.25 wt/wt and the PC specification of the bottoms increased at 0.0056 wt/wt; c: the DMC specification in the bottoms cannot be achieved with the initial two-end specifications.

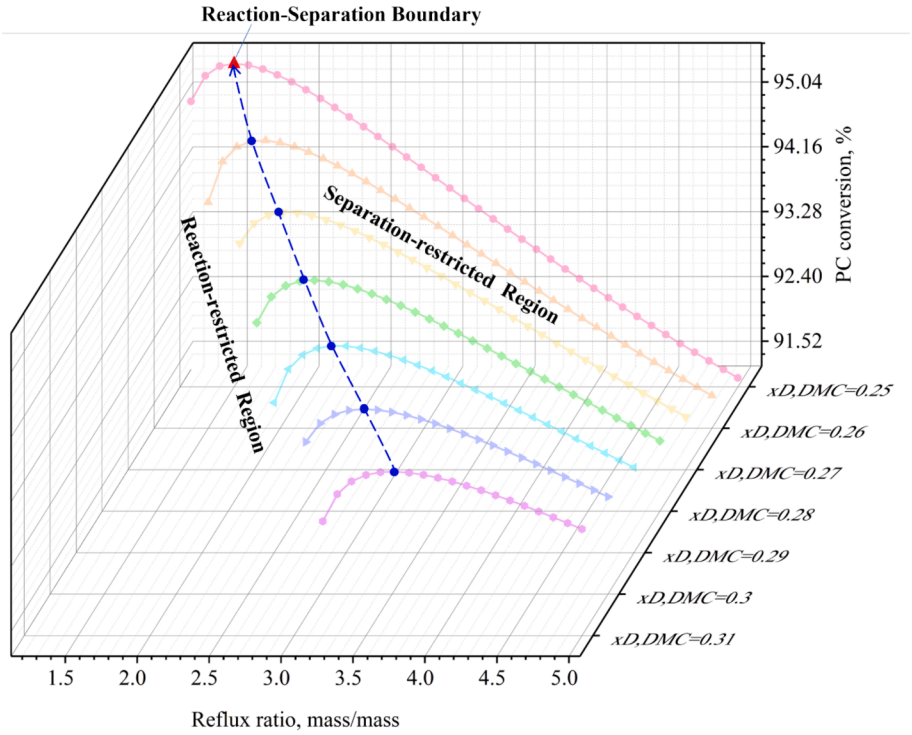


**Fig. 17.** Influences of reflux ratio on PC conversion at various distillate DMC specifications at a holdup of 1 $m^3$.

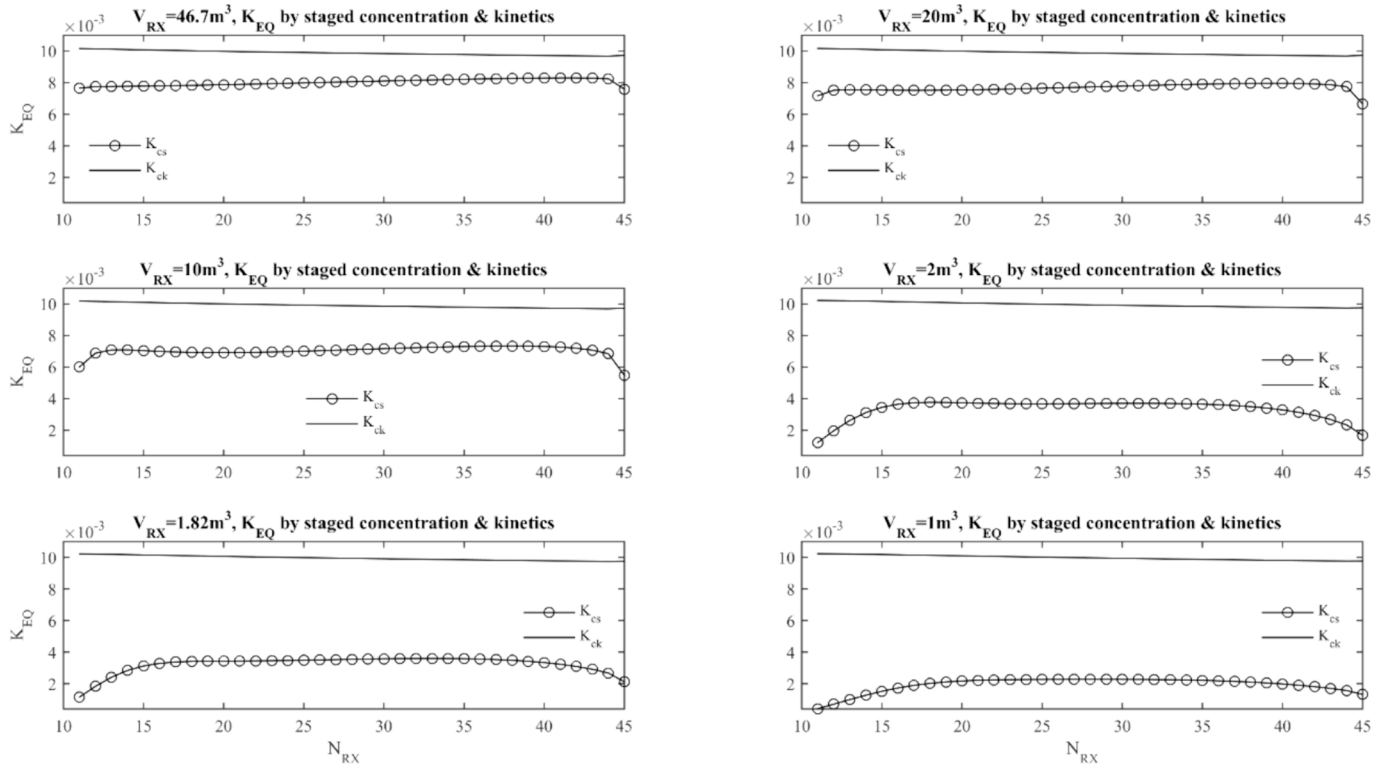


**Fig. 18.** Chemical equilibrium constant $K_{cs}$ based on staged concentration compared to the theoretical $K_c$ according to the Zhang's kinetics [23] at various holdups.

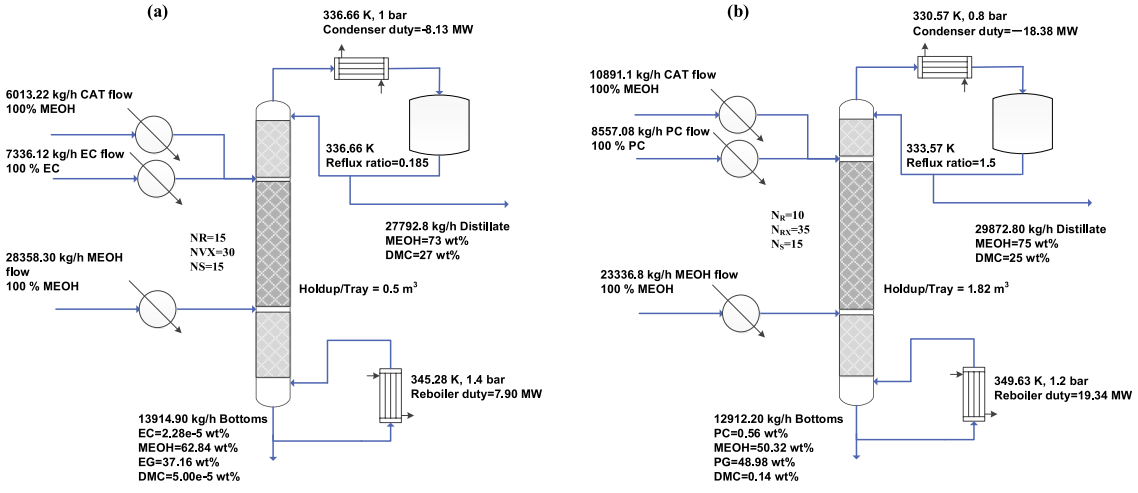


**Fig. 19.** Processes flowsheet diagram of the reactive distillation via the two routes: (a) ethylene carbonate transesterification, and (b) propylene carbonate transesterification.

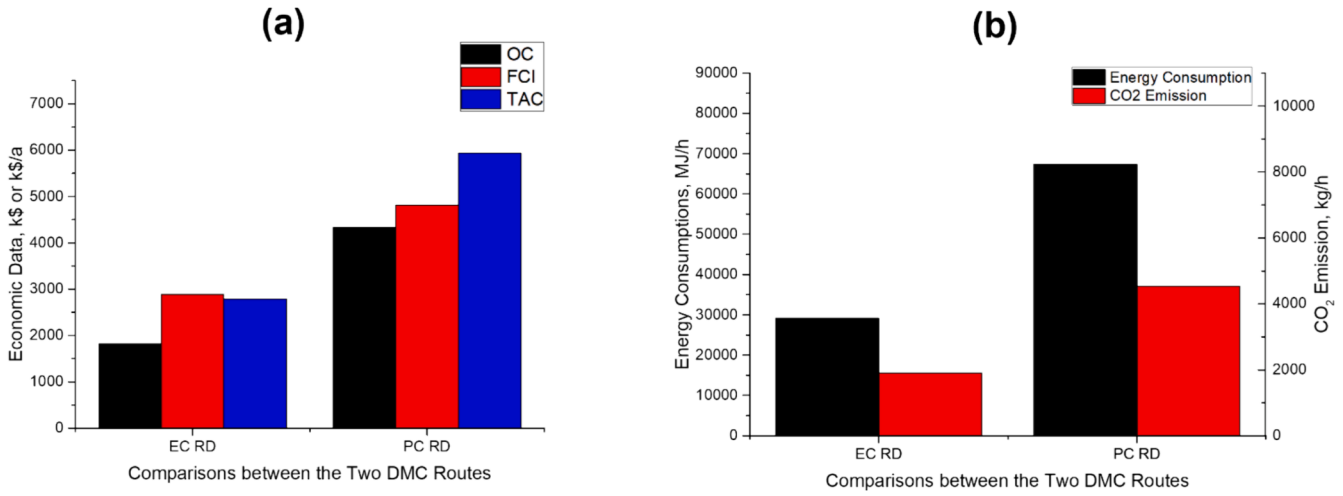


**Fig. 20.** Comparisons between the two DMC routes: (a) operating cost, fixed capital investment cost, and total annual cost, (b) energy consumption and carbon dioxide emission.

## Acknowledgments

M. Xia appreciates the assistance from the staff at the College of Chemical Engineering in Nanjing Tech University, the former colleague at Groups 610 and 620 in the State Key Laboratory of Coal Conversion, ICC, CAS. This work is financially supported by the Natural Science Foundation of China (Grant No. 21706271, 22202225, 22208361, 22208154), Natural Science Foundation of Jiangsu Province (Grant No. BK20220348) and the China Postdoctoral Science Foundation (Grant No. 2019M653488).

## Appendix A. Supplementary material

Supplementary data to this article can be found online at https://doi.org/10.1016/j.seppur.2024.129745.

## References

[1] T. Keller, J. Holtbruegge, A. Niesbach, A. Górak, Transesterification of dimethyl carbonate with ethanol to form ethyl methyl carbonate and diethyl carbonate: a comprehensive study on chemical equilibrium and reaction kinetics, Ind. Eng. Chem. Res. 50 (19) (2011) 11073–11086.
[2] Z. Huang, J. Li, L. Wang, H. Jiang, T. Qiu, Novel procedure for the synthesis of dimethyl carbonate by reactive distillation, Ind. Eng. Chem. Res. 53 (8) (2014) 3321–3328.
[3] Z.X. Huang, Y.X. Lin, X.D. Wang, C.S. Ye, L. Li, Optimization and control of a reactive distillation process for the synthesis of dimethyl carbonate, Chin. J. Chem. Eng. 25 (8) (2017) 1079–1090.
[4] Y. Zhang, Y. Zhong, Z. Wu, B. Wang, S. Liang, H. Wang, Solvent molecule cooperation enhancing lithium metal battery performance at both electrodes, Angew. Chem. Int. Ed. 59 (20) (2020) 7797–7802.
[5] D. Kim, M.Y. Lee, Y. Shin, J. Lee, J.W. Lee, Direct production of diethyl carbonate from ethylene carbonate and ethanol by energy-efficient intensification of reaction and separation, Chem. Eng. Proc.-Process Intensification (2023) 192.
[6] W. Deng, L. Shi, J. Yao, Z. Zhang, A review on transesterification of propylene carbonate and methanol for dimethyl carbonate synthesis, Carbon Resources Conversion 2 (3) (2019) 198–212.
[7] P. Kumar, V.C. Srivastava, I.M. Mishra, Dimethyl carbonate synthesis by transesterification of propylene carbonate with methanol: Comparative assessment of Ce-M (M=Co, Fe, Cu and Zn) catalysts, Renew. Energy 88 (2016) 457–464.
[8] Q.-W. Song, R. Ma, P. Liu, K. Zhang, L.-N. He, Recent progress in $CO_2$ conversion into organic chemicals by molecular catalysis, Green Chem. 25 (17) (2023) 6538–6560.
[9] J.-Y. Li, Q.-N. Zhao, P. Liu, D.-S. Zhang, Q.-W. Song, K. Zhang, Incorporation of CO2 into carbonates through carboxylation/hydration reaction, Greenhouse Gases Sci. Technol. 8 (5) (2018) 803–838.
[10] Q.-W. Song, Z.-H. Zhou, L.-N. He, Efficient, selective and sustainable catalysis of carbon dioxide, Green Chem. 19 (16) (2017) 3707–3728.
[11] S.-J. Wang, C.-C. Yu, H.-P. Huang, Plant-wide design and control of DMC synthesis process via reactive distillation and thermally coupled extractive distillation, Comput. Chem. Eng. 34 (3) (2010) 361–373.
[12] S. Fukuoka, I. Fukawa, T. Adachi, H. Fujita, N. Sugiyama, T. Sawa, Industrialization and expansion of green sustainable chemical process: A review of non-phosgene polycarbonate from $CO_2$, Org. Process Res. Dev. 23 (2) (2019) 145–169.
[13] T. Keller, J. Holtbruegge, A. Górak, Transesterification of dimethyl carbonate with ethanol in a pilot-scale reactive distillation column, Chem. Eng. J. 180 (2012) 309–322.
[14] A. Niesbach, R. Fuhrmeister, T. Keller, P. Lutze, A. Górak, Esterification of acrylic acid and n-butanol in a pilot-scale reactive distillation column—experimental investigation, model validation, and process analysis, Ind. Eng. Chem. Res. 51 (50) (2012) 16444–16456.
[15] K. Sundmacher, A. Kienle, Reactive Distillation: Status and Future Directions, John Wiley & Sons, 2002.
[16] X. Yang, X. Ma, S. Wang, J. Gong, Transesterification of dimethyl oxalate with phenol over $TiO_2/SiO_2$: Catalyst screening and reaction optimization, AIChE J. 54 (12) (2008) 3260–3272.
[17] J.B. Li, T. Wang, Coupling reaction and azeotropic distillation for the synthesis of glycerol carbonate from glycerol and dimethyl carbonate, Chem. Eng. Proc.-Process Intensification 49 (5) (2010) 530–535.
[18] I. Patrascu, C.S. Bîldea, A.A. Kiss, Novel eco-efficient process for dimethyl carbonate production by indirect alcoholysis of urea, Chem. Eng. Res. Des. 160 (2020) 486–498.
[19] T. Mathuni, J.-I. Kim, S.-J. Park, Phase equilibrium and physical properties for the purification of propylene carbonate (PC) and γ-butyrolactone (GBL), J. Chem. Eng. Data 56 (1) (2011) 89–96.
[20] H. Wang, M.H. Wang, N. Zhao, W. Wei, Y.H. Sun, CaO-$ZrO_2$ solid solution: A highly stable catalyst for the synthesis of dimethyl carbonate from propylene carbonate and methanol, Catal. Lett. 105 (3–4) (2005) 253–257.
[21] S.J. Lv, S.H. Zhang, C.J. Yang, C.J. Xu, M. Zhou, Study on simulation of synthesis of dimethyl carbonate by slurry catalytic distillation, Chem. React. Eng. Technol. 22, (6) (2006) 6 (In Chinese).
[22] C.J. Yang, L. Shao, C.J. Xu, M. Zhou, Synthesis of methyl-carbonate from methanol and propylene carbonate by slurry catalyzed distillation, Petrochem. Technol. 35 (2) (2006) 6 (In Chinese).
[23] S.G. Zhang, Y.S. Luo, Studies on the kinetics and technological conditions of the synthesis of dimethyl carbonate, Chem. React. Eng. Technol. 01 (1991) 10–19 (In Chinese).
[24] Y.J. Fang, W.D. Xiao, Experimental and modeling studies on a homogeneous reactive distillation system for dimethyl carbonate synthesis by transesterification, Sep. Purif. Technol. 34 (1–3) (2004) 255–263.
[25] A. Haznan, Studies on kinetics of dimethyl carbonate synthesis by homogeneous transesterification, *Indonesian J. Appl. Chem.* 11 (2) (2009).
[26] Y.J. Fang, D.J. Liu, A reactive distillation process for an azeotrople reaction system: transesteirification of ethylene carbonate with methanol, Chem. Eng. Commun. 194 (10–12) (2007) 1608–1622.
[27] Y. Shi, H. Liu, K. Wang, W. Xiao, Y. Hu, Measurements of isothermal vapor–liquid equilibrium of binary methanol/dimethyl carbonate system under pressure, Fluid Phase Equilib. 234 (2005) 1–10.
[28] H.-P. Luo, W.-D. Xiao, K.-H. Zhu, Isobaric vapor–liquid equilibria of alkyl carbonates with alcohols, Fluid Phase Equilib. 175 (1) (2000) 91–105.
[29] H.-P. Luo, J.-H. Zhou, W.-D. Xiao, K.-H. Zhu, Isobaric vapor−liquid equilibria of binary mixtures containing dimethyl carbonate under atmospheric pressure, J. Chem. Eng. Data 46 (4) (2001) 842–845.
[30] Y.-J. Fang, J.-M. Qian, Isobaric vapor−liquid equilibria of binary mixtures containing the carbonate group −OCOO−, J. Chem. Eng. Data 50 (2) (2005) 340–343.
[31] Asahi Kasei, J. Process for industrial production of dialkyl carbonates and diols. WO 2007/060893 (Nov. 25, 2005), May 31, 2007; JP 4246779 B2, Apr. 2, 2009., Nov. 25, 2005.

[32] A. Rodríguez, J. Canosa, A. Domínguez, J. Tojo, Vapour–liquid equilibria of dimethyl carbonate with linear alcohols and estimation of interaction parameters for the UNIFAC and ASOG method, Fluid Phase Equilib. 201 (1) (2002) 187–201.
[33] M.S. Ding, Liquid−solid phase equilibria and thermodynamic modeling for binary organic carbonates, J. Chem. Eng. Data 49 (2) (2004) 276–282.
[34] N. Cheng, Solvents Handbook, 3rd ed.;, Chemical Industry Press, Beijing, 2002.
[35] https://webbook.nist.gov/chemistry/. In NIST Chemistry WebBook: 2024-7-17.
[36] S.-B. Hung, M.-J. Lee, Y.-T. Tang, Y.-W. Chen, I.K. Lai, W.-J. Hung, H.-P. Huang, C.-C. Yu, Control of different reactive distillation configurations, AIChE J. 52 (4) (2006) 1423–1440.
[37] Y.-T. Tang, Y.-W. Chen, H.-P. Huang, C.-C. Yu, S.-B. Hung, M.-J. Lee, Design of reactive distillations for acetic acid esterification, AIChE J. 51 (6) (2005) 1683–1699.
[38] M.A. Al-Arfaj, W.L. Luyben, Plantwide control for TAME production using reactive distillation, AIChE J. 50 (7) (2004) 1462–1473.
[39] K.J. Huang, S.J. Wang, Design and control of a methyl tertiary butyl ether (MTBE) decomposition reactive distillation column, Ind. Eng. Chem. Res. 46 (8) (2007) 2508–2519.
[40] W.L. Luyben, C.C. Yu, Reactive Distillation Design and Control, John Wiley & Sons, Hoboken, New Jersey, 2008.
[41] J.M. Douglas, Conceptual Design of Chemical Processes, McGraw-Hill Chemical Engineering, New York, 1988.
[42] W.L. Luyben, Principles and case studies of simultaneous design, John Wiley & Sons, Hoboken, 2012.
[43] T. Shi, W. Chun, A. Yang, Y. Su, S. Jin, J. Ren, W. Shen, Optimization and control of energy saving side-stream extractive distillation with heat integration for separating ethyl acetate-ethanol azeotrope, Chem. Eng. Sci. 215 (2020) 115373.
[44] M.A. Gadalla, Z. Olujic, P.J. Jansens, M. Jobson, R. Smith, Reducing $CO_2$ emissions and energy consumption of heat-integrated distillation systems, Environ. Sci. Tech. 39 (17) (2005) 6860–6870.
[45] A. Yang, S. Sun, A. Eslamimanesh, S.A. Wei, W. Shen, Energy-saving investigation for diethyl carbonate synthesis through the reactive dividing wall column combining the vapor recompression heat pump or different pressure thermally coupled technique, Energy 172 (2019) 320–332.